AN ABSTRACT OF THE THESIS OF

James J.Fuller for the degree of Masters of Science in Forest Products presented on April 6, 1990.

Title: Predicting the Thermo-Mechanical Behavior of A Gypsum-To-Wood Nailed Connection

Signature redacted for privacy.

Abstract approved: _____
Robert J. Leichti

With high costs of testing and rating a structural system for fire resistance, the utilization of computer simulations that approximate the integrity of structural subsystems could conceivably reduce development costs. Before an analysis of a light-frame wood system can occur, information on the components of the substructure must be known. The purpose of this study was to systematically study the effects of thermal load on the strength and mode of failure in a nailed gypsum-to-wood stud connection.

Initially the distribution of temperatures within the connection was sought by using a finite element analysis. The analysis simulated exposure to a standard fire as dictated by the American Society for Testing Materials standard E-119. The thermal properties of the materials involved are documented in the

literature. Close agreement was found between analytical results and specimens exposed to standard test conditions.

With the temperatures along the connection known, the properties of the three materials at elevated temperatures were needed. For wood and steel, this information has been well documented. The property values for gypsum were accumulated through testing gypsum board in compression at various temperatures. The results showed an increase in compressive strength and stiffness up to 100 C followed by a decrease in strength. These results were combined with the analytically determined temperature distribution to obtain the material properties in the neighborhood of the connection.

The overall model was an extension of the yield theory available in the literature. The approach used was to evaluate the connection at set time intervals and calculate the strength of the connection. Each time interval had a different set of material property values for each material in the connection as dictated by the temperature distribution. The mode of failure did not change from that which occurred at room temperature, compression strength of the gypsum being the determining factor. The load at which failure occurred increased in the first five minutes and then sharply decreased. This can now be incorporated into models of wall systems for room temperature to predict behavior of walls during exposure to fire.

Predicting the Thermo-Mechanical Behavior of A Gypsum-To-Wood Nailed Connection

by

James J. Fuller

A Thesis

submitted to

Oregon State University

in partial fulfillment of
the requirements for the
degree of

Masters of Science

Completed April 6, 1990
Commencement June 1990

APPROVED:

Signature redacted for privacy.

Assistant Professor of Forest Products in Charge of Major

Signature redacted for privacy.

Head of Department of Forest Products

Signature redacted for privacy.

Dean of Graduate School

Date thesis is presented April 6, 1990

ACKNOWLEDGEMENTS

The author thanks Dick Holbo for assistance with the instrumentation and David LaFever for fabricating the testing hardware. Recognition is due Robert White from the USDA Forest Service, Forest Products Laboratory in Madison, Wisconsin for exposing the wall assemblies to fire conditions.

Also, thanks goes to Robert Leichti as the author's major professor for his guidance, advice, and continued patience in taking an illiterate carpenter and trying to transform him into a scholar.

A special note of appreciation goes to the author's family for providing many bright spots after long hard days and nights when it seemed like nothing was accomplished. The author extends a special thanks to his wife, for she had the dubious honor of having the first whack at his papers with the red pen.

Funding for this project was provided by Manasha Corporation through the Dick Hansen Fellowship, the Mary McDonald Fellowship, and the Center for Wood Utilization, Department of Forest Products, Oregon State University.

TABLE OF CONTENTS

LIST OF FIGURES

LIST OF FIGURES
continued

LIST OF TABLES

Predicting the Thermo-Mechanical Behavior of A Gypsum-To-Wood Nailed Connection

I. INTRODUCTION

Light-frame construction where wood is the principal structural material, is the most common type of construction design for residential structures in the United States and is frequently found in single and multi-story commercial and industrial buildings. This is because minimal engineering design is needed; the designer can refer to easily understood design specifications in standard building codes. As a general definition, light frame construction relies on nominal 2-inch lumber for the framing members and various materials for the sheathing. The vertical members within the walls, called studs, are 2-by-4s with 2-by-6s becoming more common. The studs are placed 41 and 61 cm apart on center to conform to standard sheathing materials which are produced with their lengths in multiples of 122 cm. Plywood is a typical material for exterior sheathing with gypsum board being the most frequently used on the interior.

Gypsum board, also referred to as sheetrock or drywall, can serve three functions. First, it provides a substrate for decorative materials. Second, gypsum board provides protection of the framing members from fire damage. Although one layer of regular gypsum does not have fire resistance rating as high as Type-X gypsum, it is rated for fire resistance (White 1982; Sherwood and

Moody 1989). The third function, as with all sheathing, is to provide structural rigidity to resist lateral loads.

Without the exterior and interior sheathing the frame has no lateral stability. It is the connections between the framing and sheathing which transfer lateral forces, such as those applied by earthquakes, wind loads, and in-plane buckling, to the sheathing which in turn provides the rigidity to the wall system. The most common form of gypsum-to-stud connection is the wire nail.

In 1988, 56% of the property loss of fires were residential buildings (NSC 1989). In the previous years in which the total number of fires increased, residential building fires accounted for the increase. While the structural performance of light-frame construction is widely accepted for ordinary service loads, fire performance of the system is the focus of extensive and elaborate full-scale testing. Under fire loading, the structure is subjected to ordinary service loads as well as the thermal load of the fire. It is during fire loading that the materials of the framing system, ie, wood, nails, and gypsum, experience severe degradation conditions. At the same time that additional mechanical stresses are applied, each of these materials may be loosing strength and stiffness.

Under the combined thermal and service loads, the framing connection is subjected to a combination of mechanical and thermal loads. The thermal load is dynamic and changes with fire

conditions. The exposure to high temperatures leads to degradation of the materials in the joint and hence the mechanical integrity of the joint.

At the present time, design professionals rely on established fire ratings which assign a degree of fire resistance as opposed to fire proofing. No building is fire proof, only fire resistant, even buildings of concrete. This condition arises because all materials degrade at high temperatures which may cause structural failure. Presently, fire ratings of structural systems are based on experimental studies as specified by the American Society for Testing and Materials (ASTM) standard E-119. These studies are expensive, time consuming, and the information obtained is limited in scope. New structural systems cannot be rated on past testing within this practice. Building codes and labeling systems require the same extensive testing with each minor change in the materials or construction detail. As an example, the Gypsum Association (1988) publishes the Fire Resistance and Sound Control Manual. The manual presents descriptions and ratings for forty wall systems not including floor and ceiling systems. Each of these designs had to be tested separately for fire resistance.

Inspection of the problem suggests that ultimately the analysis of the structural systems under fire and service loadings is needed. However, several critical components of the structural performance under the named loading conditions must be

characterized. One of these critical components is the light-frame joint formed by the gypsum wall covering material, the nail, and the wood stud.

The objective of this project was to determine the strength of the joint when exposed to a standard fire. The framing materials forming the joint degrade at different temperatures. To further complicate the problem, each material in the joint experiences different rates of temperature rise. With these differences, it is not known when the joint will fail, or which material will fail first if there are no simultaneous failures. If a basic joint and material property data base was developed, the information could be used in computer simulations to evaluate new system designs. Fire ratings could then be assessed by computer without total reliance on expensive and elaborate testings.

The problem solution was approached by integrating analytical and experimental activities. Figure 1 shows the flow of the activities that were followed. First, the mechanical properties of the three materials were determined as a function of temperature. Then the temperature distribution about the joint as a function of time was established. Finally the results of the first two activities were used to predict the strength of the joint as a function of time.

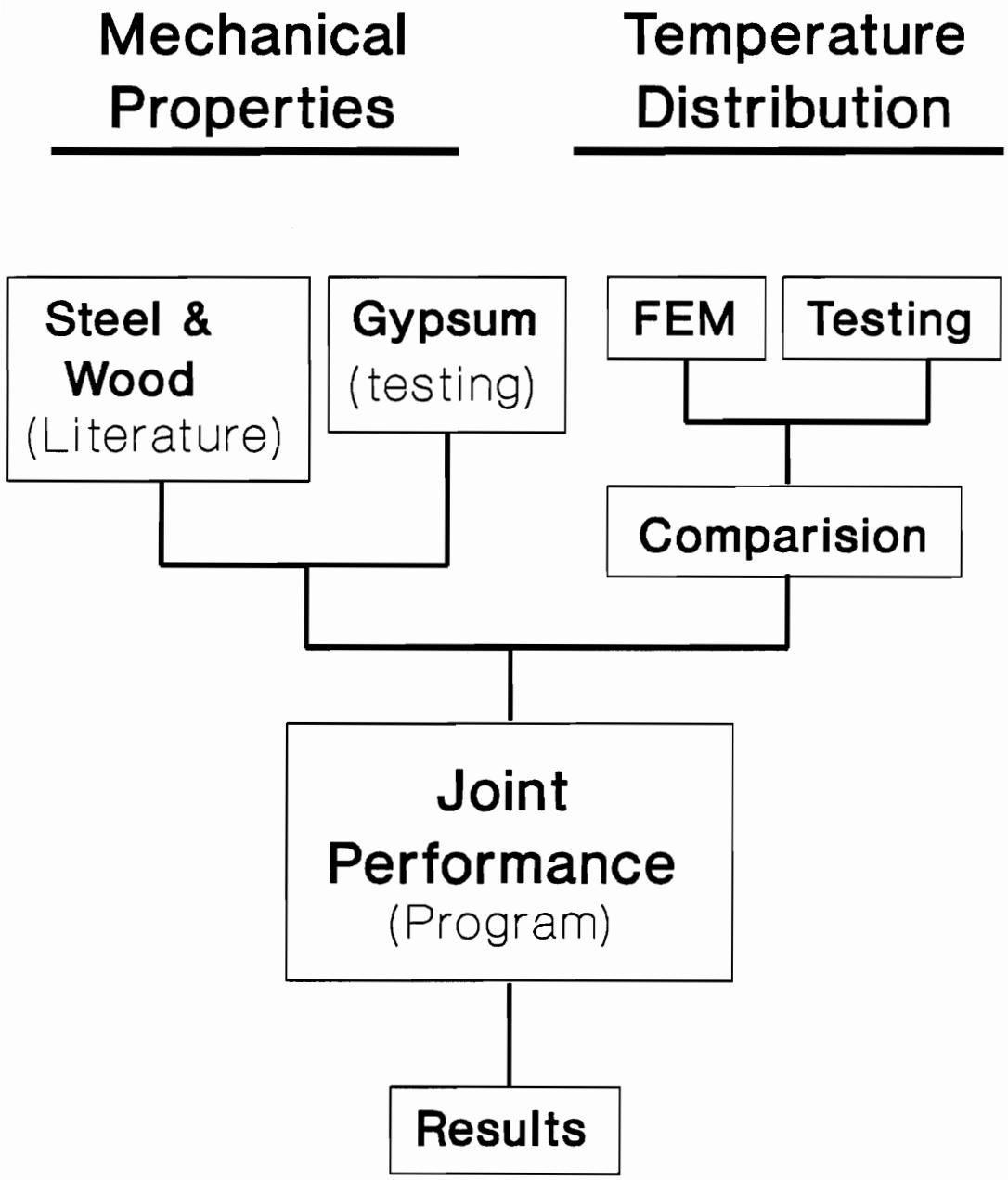

Figure 1. Flow Chart of the Study

II. LITERATURE REVIEW

The joint between the stud and sheathing provides resistance to in-plane buckling and racking attributable to seismic and wind loads. As shown in Figure 2, the joint is composed of three different materials. Performance has been evaluated statically and dynamically but is further complicated by the superposition of thermal loads such as fire. The complexity is a result of different material characteristics at elevated temperatures.

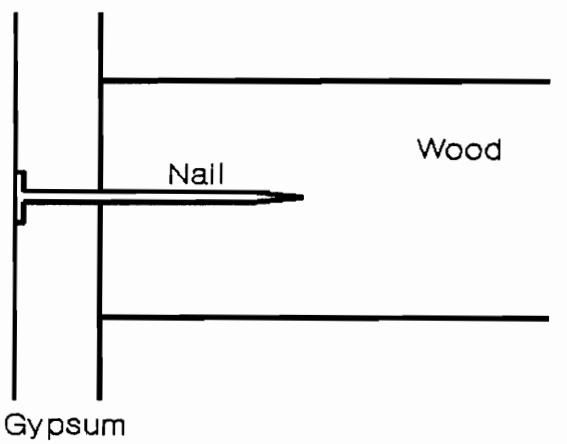

Figure 2. Characteristic Mechanical Connection Between Gypsum Board and Wood Stud in Light-Frame Construction

The literature review presents the necessary background and literature in four main areas. The initial discussion reviews approaches previously used in similar problems, followed by the discussion of the load imposed by fire. Changes in mass and heat due to elevated temperatures and changes that affect mechanical properties are then discussed. Finally, consideration is given to available empirical models used to describe the joint behavior.

Approaches Previously Used

Approaches used in the past have ranged from experimentally determining the performance of a structure to combining experimental results with a computer simulation. Avent and Issa (1984) predicted time to failure of epoxy repaired timbers by exposing samples to fire. Jeanes (1985) used experimental results to confirm predictions generated from a computer model of steel framed buildings. Chang (1986) incorporated previously gathered material data into his computer simulations of wooden bends. He then determined the strength and stiffness of wooden bends exposed to constant elevated temperatures.

Fire Load

The three means of heat flow are conduction, convection, and radiation. However, in the case of fire, convection and radiation are the principal mechanisms of heat transfer (Harmathy 1977, 1976

by Sherwood and Moody 1989). Of these, radiation is the primary form of heat flow between the source and the receiver. Therefore, fire simulation models can ignore conduction and convection.

The American Society for Testing Materials (ASTM 1988) test for fire exposure specifies that failure occurs when one of the following happens: 1) the system or member collapses, or 2) the flames or heated gases are able to penetrate the system. It also specifies the temperature of the furnace gases rather than the heat flow to the object to be tested. The time-temperature relationship is presented in Figure 3. In modeling ASTM E-119, radiant heat flow can be estimated by using an equation based on the temperatures of the source and receiver. The equation used was (Swanson 1988)

$$q = s\ V\ A\ e\ (T_1^4 - T_2^4) \qquad [1]$$

where

s = Stefvan-Boltzman constant ($5.676\ 10^{-8} w/m^2K^4$)
V = view factor
A = area of exposure (m^2)
e = equivalent emissivity and absorptivity
T_i = temperature (C)
q = heat flow (w)

The view factor is a function of distance and exposure angle between the heat source (combustion gases) and receiver (wall). The average view factor for the wall geometry is .6 on a scale of 0 to 1 (Gammon 1987).

The emissivity and absorptivity of the heat source is affected by the temperature of the receiver as well as the composition,

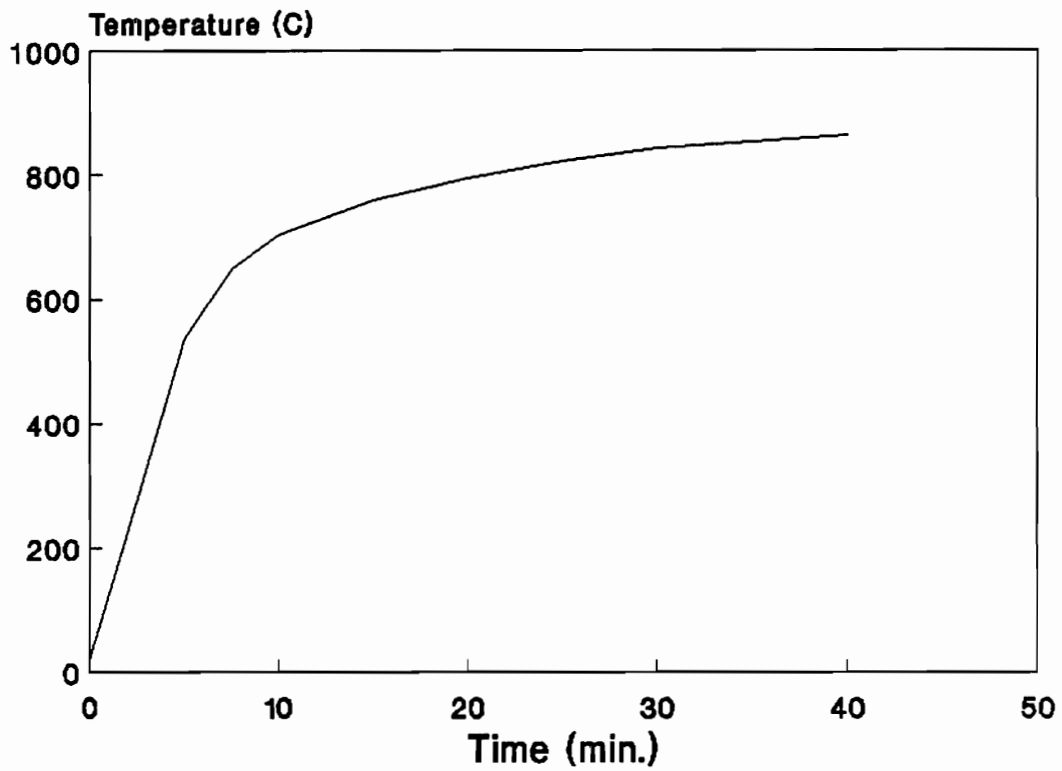

Figure 3. Standard Time and Temperature Curve for ASTM E-119

density, and wave length of the heat source. The emissivity and absorptivity of the receiver is influenced by the surface condition of the receiver and the temperature of the heat source. On a scale of 0 to 1, Gammon (1987) reported an effective emissivity is .7.

Within the joint, conduction is a primary form of heat transfer. The governing equation is (Swanson 1988)

$$\rho C_p(\partial T/\partial t) = \partial/\partial x\ (k_{xx}\ \partial T/\partial x) + \partial/\partial y\ (k_{yy}\ \partial T/\partial y) + \partial/\partial z\ (k_{zz}\ \partial T/\partial z) \quad [2]$$

where

ρ = density (kg/mm^3)
C_p = specific heat (J/Km^3)
k_{ij} = thermal conductivity (w/mmK)
t = temperature (K)
x,y,z = geometric coordinates (mm)

Changes in Wood

Chemical Make-Up and Thermal Properties

When a wood sample is exposed to elevated temperatures, four pyrolytic stages are identified, and these are usually categorized into temperature ranges which coincide with distinct physical and chemical reactions.

The first stage is usually delineated by the range of temperatures from 20 to about 200 C. In this stage, the rate of heating plays a role in the process. If heating proceeds slowly (Schaffer 1973; White and Schaffer 1980) all free and bound water is expelled to the atmosphere by the time 105 C is reached. However, White and Schaffer (1980) indicates that if the process is rapid, some water may be driven internally by a local pressure gradient whereupon it condenses and preheats the wood. As the temperature wave progresses through the wood, the point of the highest moisture content is found where the temperature is about 100 C. This peak in moisture content may be as high as twice the initial value. If this moisture is in bound form, it must gain the heat of vaporization,

570 cal/g (Skaar 1978), as well as bound energy before it can evaporate again. The absorption of energy for moisture vaporization helps to reduce the rate at which temperature increases in the surrounding material.

If the wood is dry, all three major constituents of wood hemicellulose, lignin, and cellulose, are stable under 110 C (Beall and Eickner 1970). Above this temperature they list water of constitution, carbon dioxide, and acetic acid as non-combustibles volatles that are lost. Furthermore, they state that hemicellulose begins to pyrolyze at 180 C and may have a glass transition at 55 C, whereas Lignin has a glass transition at 120 C (Schaffer 1973) and rehardens at 160 C (Beall and Eickner 1970). If the wood has an initial moisture content, all components degrade sooner than when moisture is absent (Goring 1963).

The second pyrolytic stage occurs from 200 to 288 C. At 200 C, lignin again begins to soften (Goring 1963) or undergo an exothermic reaction and at 250 C begins to rapidly break down (Beall and Eickner 1970). Cellulose dehydrates at 200 C and depolymerizes at 210 C (Schaffer 1973).

The third stage begins at approximately 288 C where rapid weight loss occurs, char forms, and volatile gases evolve. Rate of weight loss rapidly decreases above this temperature. The actual temperature at which charring occurs is a function of thickness of the char which has already developed and time of exposure to

elevated temperatures (Blackshear and Murty 1965). The char base temperature, also called pyrolytic temperature, has been measured at 350 C at the surface and 150 C at the interior points (Blackshear and Murty 1965). Longer dwell times in the lower temperature ranges cause a lowering of the temperature at which the third pyrolytic stage will occur.

The rate of temperature rise is dependent on the heat source, diffusivity, and the distance a point is from the heat source (Kanury 1972b, 1973; Kansa 1977). The two extremes of this rate of temperature rise can be identified. In the first case, the temperature rise is governed by the amount of heat generated. This is when a point of consideration is close to an intense heat source and while the diffusivity of the material is low then . This produces a narrow zone of pyrolysis. The other extreme would be, if a point of consideration is distant from a moderate heat and the diffusivity of the material is high, then the temperature rise is governed by the internal convection of pyrolysis gases and the char properties. This produces a wide zone of pyrolysis.

The fourth pyrolytic stage starts in the range of 440 to 600 C, all volatiles from the area have been lost and only char and ash remain. However, volatiles from other areas can be transported through this char layer (Kanury and Blackshear 1970b). Here a better criteria than temperature maybe density since the actual temperature may vary (Kanury and Blackshear 1970).

The char layer is primarily the product of pyrolyzed lignin rather than hemicellulose and cellulose. Approximately 50% of the lignin turns into char, whereas only 10% of the cellulose turns into char (Roberts and Clough 1963). In this stage, the char surface reacts with oxygen in glowing combustion which is highly exothermic. In our analytical study, the joint will not be exposed to oxygen, and the exothermic reaction will not be considered. However, the analysis will include the possibility of a non-combustion char layer.

The time at which a char layer does develop depends on factors varying within and between wood species such as: moisture content, permeability, density, heart wood content, and rate of volatiles released which is a function of char depth (Schaffer 1967). Of the many char rate models developed, Schaffer (1967) developed an empirical model, and Kanury (1972) developed a theoretical model. The model Schaffer (1967) proposed is shown in equation [3]

$$t = ((a + b\,MC)\,SPGR + c)\,x \qquad [3]$$

where

t = time (hr)
x = char depth from original surface (in.)
MC = moisture content (%)
SPGR = specific gravity
a,b,c = regression constants

Table 1 has some of the constants for Schaffer's model. These are for exposure of an open surface for ASTM E-119 and reflects the differences in density, permeability, and moisture content.

Table 1. Char Equation Constants for Wood From Schaffer (1967)

Wood	a	b	c
Douglas-fir	28.726	.578	4.187
Southern Pine	5.832	.12	12.862
White Oak	20.036	.403	7.519

Whether or not all the reactions during the fourth pyrolysis stage are exothermic or endothermic has been debated to a great extent. The endothermic argument explains the reaction as the heat of vaporization of the material when no oxygen is present (Kanury 1973). The exothermic argument requires that cellulose serve as an autocatalyst, thereby not needing the presence of gaseous oxygen (Kuber 1982; Roberts and Clough 1963).

During pyrolysis, primary and secondary exothermic reactions take place but are of different magnitudes (65 cal/gm, 85 cal/gm) (Roberts and Clough 1963). These values occurred during a temperature rise of 20 C/min. above 320 C. The magnitude of heat created is governed by two geometric factors; how near the point of

concern is to the surface, and the presence of char layer fissures. These two factors govern the residence time of the vapors within the wood near the cellulose catalyst. Therefore, the vapors react more completely to generate more heat. There are numerous reports that include exothermic values which closely agree.

When the rate of heating is increased to within the range of 20 C/ min to 50 C/min, quite different results occur (Beall and Eickner 1970). The heat of reaction is not sensed until a higher temperature. The form of the reported data is in "apparent specific heat." Apparent specific heat includes the heat of reaction by lowering the externally applied heat needed to raise the temperature when an exothermic reaction occurs (Harmathy 1983). As an example, the values for wood are shown in Figure 4.

Mechanical Properties

Most studies dealing with compression have been below 100 C because the primary concern was with the exposure temperatures for drying wood. Unlike tension, compression does not depend greatly on the integrity of cellulose. Rather, compressive strength depends on the structure of hemicellulose and lignin (Schaffer 1973). As was stated earlier, hemicellulose in dry wood starts to soften at 80 C. Quickly after this, compression strength begins to decrease. At 120 C lignin begins to soften and the wood continues to decrease in compressive strength. At 160 C, lignin rehardens and the

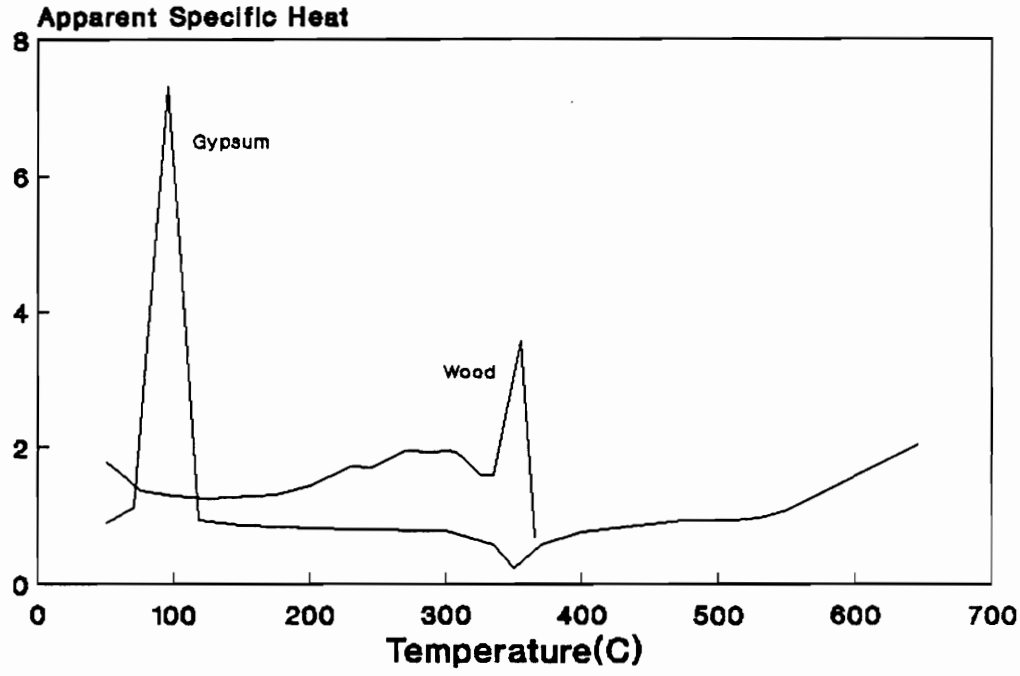

Figure 4. Comparative Apparent Specific Heats of Wood and Gypsum

compressive strength becomes constant until 200 C. Then the compressive strength declines at an accelerating rate up to 288 C where 15% of its room temperature strength remains. The formation of phenolic resin bonds in the lignin during encrusting has been used to explain the plateau in compression strength (Harkin 1969 by Schaffer 1973).

Stress and strain failures can be correlated to the load and temperature history (Schaffer 1973). In the work by Schaffer (1973), two loading regimes were used. One was loading to failure

at a rate of .09 cm/cm/min. The second was first subjected to a 2-hour sustained loading below failure then followed by loading to failure at a rate of deformation the same as the first group. In the first group, total strain decreased at higher temperatures. With a sample that had a sustained load and then experienced increased load until failure, a slightly different sequence occurred. Up to 93 C, the sustained stress follows the trend of the first group's ultimate stress. From 93 C, total strain increased until 150 C, and compressive strength displayed a less dramatic decrease than the first group. It follows, that if compressive strength was affected by an increased number of phenolic bonds in lignin, and if these bonds remained after cooling, then the increased strength should remain. This was observed as a 10% increase in strength. After cooling, samples that were heated in the range 100 to 288 C greater compressive strength. Furthermore, recovery of deformation was greater with sustained loads as opposed to high speed ramping (Schaffer 1977).

As a result, physical changes can be correlated to four distinct temperatures associated with changes in hemicellulose and lignin. Hemicellulose softens at 80 C, lignin softens at 120 C, lignin rehardens at 160 C, and lignin softens or goes through an exothermic reaction at 200 C (Schaffer 1973; Berkowitz 1957; Beall and Eickner 1970; Goring 1963). The effects are shown in Figure 5.

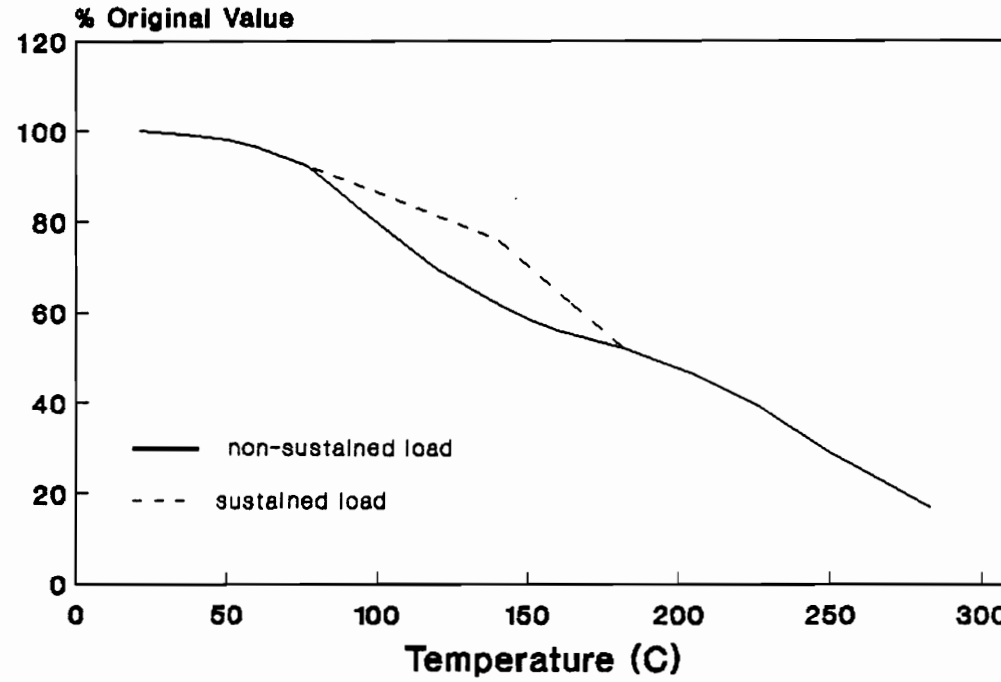

Figure 5. Compressive Strength of Wood as a Function of Temperature

If the wood is not initially dry, the response to elevated temperatures is different. At 12% moisture content, the initial decrease in strength is more rapid and then slows at 70 C until 140 C where it displays greater compressive strength than the oven-dry samples. At 288 C, similar strengths again were obtained (Schaffer 1977). One report which used a temperature controlled water bath to test at elevated temperatures, had a linear response to temperature (Sano 1961). This resulted in an 80% strength reduction at 80 C. Obviously, the moisture content had some effect.

All of the mentioned temperature effects on wood have been directed toward longitudinal compression. No data was found on either radial or tangential compression strength as exposed to fire. At room temperature, radial and tangential compression strength is approximately one tenth that of longitudinal orientation.

Changes in Gypsum

A recent literature review by Mahaffey (NAWPFRC 1989) indicates inconsistency in reported material values for gypsum board. Furthermore, he does not state what type of gypsum for which the data are reported. However, Lawson (1977) specifically states what material the values correspond to. Therefore, values from Lawson (1977) are be used in this discussion.

Chemical Make-Up

Gypsum or sheetrock is a generic term for numerous products. What they all have in common is that the main component is hydrous calcium sulphate ($CaSO_4:2H_2O$), called dihydrate, a crystalline mineral. These products may contain sand, vermiculite, glass fibers, starch, and water repellents with paper or vinyl face and back (Lawson 1977). The mechanical properties of the board are partly dependent upon the additives. The most commonly used board is regular 12.7 mm gypsum board with paper face and back and no additives. Although Type-X gypsum board is specifically designed to

be a fire barrier, most gypsum boards are adequate to provide some amount of fire resistance (White 1982; Sherwood and Moody 1989). Sherwood and Moody (1989) list several systems tested by different agencies specifying the fire resistance rating of regular gypsum. Gypsum is fire resistant partly because the only combustible component is the surface coverings (paper or vinyl) which represents a small percentage of the product. Also, the high moisture content absorbs a large quantity of heat.

Similar to wood, gypsum also exhibits discrete stages of decomposition. Lawson (1977) gives a comprehensive review of the chemical changes of gypsum. Just as wood is hygroscopic, so is gypsum. The moisture is chemically combined with calcium sulphate to form the crystalline structure. The free and bound moisture must be evaporated before the gypsum will attain a temperature above 100 C. At 100 C to 150 C the moisture of crystallinity approximately 75 % of the total water is lost which causes, the hemihydrate, plaster of paris ($CaSO_4$:$1/2H_2O$) to form; this process is called calcination (Windholz 1977). Two things occur as a result of water loss. First, the portion of the board behind the dehydration front and the stud behind the board remain cooler for a longer period of time due to the increase in the apparent specific heat which causes the board to absorb more heat. The second result is that as the board loses moisture the structural integrity degrades.

When calcination occurs in Type-X gypsum board, the glass fibers form a matrix to help retain the structural integrity (Lawson 1977). The glass fibers increase the compression strength. At 360 C, the gypsum further degrades into an insoluble form. At 1227 C, the board degrades into calcium oxide (CaO) and sulfur trioxide (SO_3).

Thermal Properties

Thermal conductivity of gypsum is dependent on the density. Gammon (1987) reported the linear relationship

$$k = .0811 + .00484\ d \qquad [4]$$

where

k = thermal conductivity (w/mK)
d = density (kg/cm^3)

For the relationship between conductivity and temperature, the following values have been reported: .25 W/mK below 100 C and .13 W/mK above 200 C for 673 kg/m^3 (Harmathy 1983). Reported specific heats as a function of temperature are shown in Figure 4. The deviations from 880 J/kgK are due to dehydration and calcination (Harmathy 1983).

Changes in Steel

The material in the nail used to mount gypsum board is cold-worked low carbon steel (Wolf 1988). Within the temperature range of the ASTM E-119 test, no chemical changes occur in steel. However, the yield strength of steel changes with temperature. Figure 6 shows the temperature - yield strength relationship (Boyes and Gall 1985). From room temperature, there is a slow decrease until about 200 C. Then at 370 C a peak is followed by a sharp decrease.

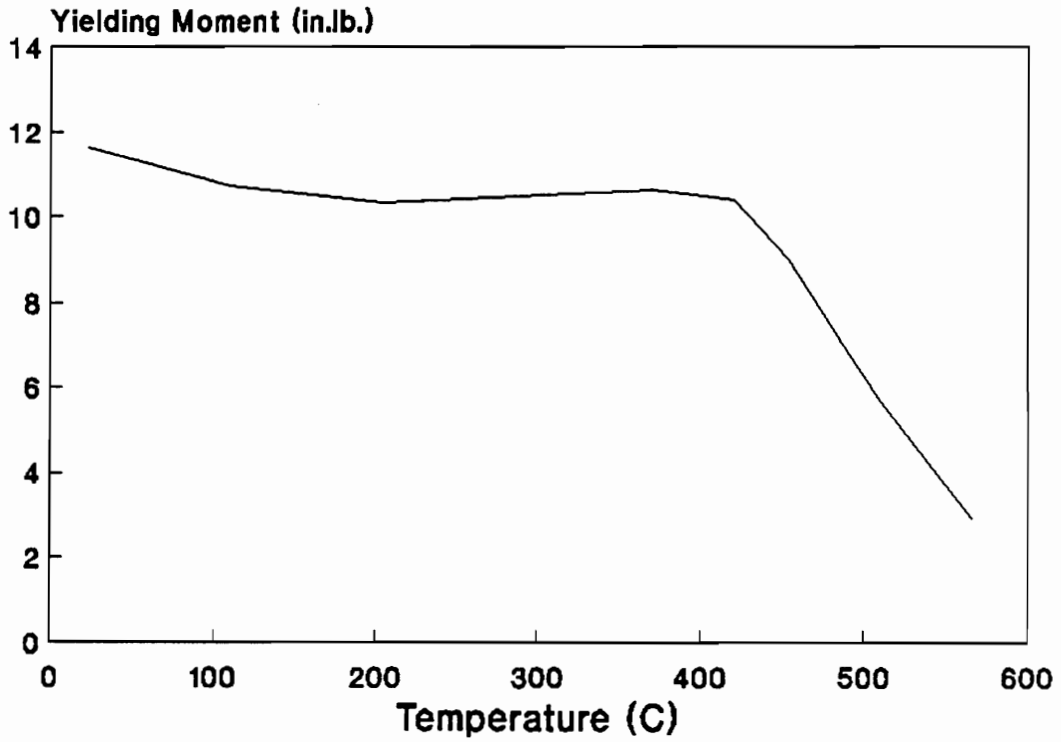

Figure 6. The yield Strength of Low Carbon Steel as a Function of Temperature (Boyes and Gall 1985)

Performance of Joints

Various theories have been proposed to describe mechanical performance of a nail joint. The two used most extensively are beam on an elastic foundation and yield theory.

The beam on an elastic foundation theory is essentially a loaded beam supported on a foundation that reacts elastically as a load is applied on the beam. Hetenyi (1946) discussed elastic bearing analysis for various load cases. Included in this is the derivation for the case in which both the elastic modulus of the beam and the elastic foundation are continuously variable. When the gypsum, nail, and wood degrade with increased temperature, the case with varying properties would be appropriate.

Yield theory compares the embedment strengths and thicknesses of the side (gypsum) and main (wood) members to the yield moment of the beam (nail) to predict the mode of failure and yield force. If all the materials are truly plastic, this method produces reasonable results with equations that are relatively simple. The assumption for failure is that once a small displacement occurs, failure is eminent. Currently the yield theory is the basis of many European codes for lateral bearing capacities of nail joints. With the current push to unify the approaches used worldwide, this country has been urged to accept the yield theory method (Aune and Patton-Mallory 1986a).

Using yield theory, the behavior is best looked at on a stress-strain diagram. Figure 7 shows how material performance can be divided into three main regions. The first is the elastic region in which the displacement is linearly related to the stress applied. The third region is failure where the material can not support the level of stress already applied. The second is the plastic or yield region where no additional stress is required to obtain additional displacement. The failure region follows the plastic region. The yield theory gives the ultimate stress that can be applied to the joint, hence, the stress at yield is also the ultimate stress. In the cases of concern here, i.e. racking or in-plane buckling, the stresses increase quickly with slight displacements.

A sheetrock nail which is usually made of steel is an example of plastic performance. Wood does not exactly conform to plastic behavior. However, studies have shown that the degree of departure of wood from the plastic behavior is insignificant and therefore can be considered as plastic (Aune and Patton-Mallory 1986).

When using the yield theory to predict failure in a joint, various modes or types of failure can occur. The modes of failure that are of interest to this study are depicted in Figure 8. Though there are various modes of failure, there are only two ways in which materials can fail. Failure of the side and main members can occur when the nail compresses them, and this property of the side and main members is called the embedment strength. However, the

materials also can fail if the nail yields, in which case the moment applied to the nail is greater then the nail can resist.

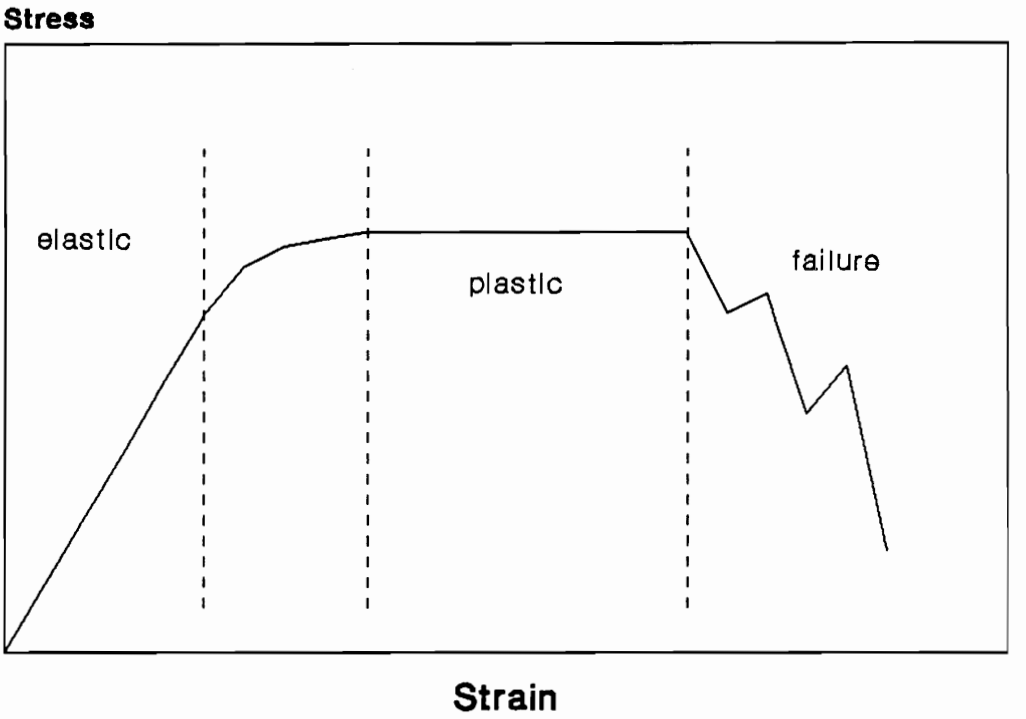

Figure 7. Ideal Elasto-Plastic Stress-Strain Curve

Depending on whether the nail or the materials which the nail is joining fail first, one can decide which mode of failure governs and the ultimate force that is necessary for failure to occur. In making this decision, the yield moment of the nail, is compared to

the maximum moment possible based on the embedment strength of the materials being joined. If the material properties, bending strength and embedment strengths, are constant or even a simple function along the length of the joint, the equations for the failure force and determination of failure mode are straight forward. The case of constant properties is given in Aune and Patton-Mallory (1986). If the material properties are more complex, the governing factors remain the same, but the equations become more complicated. In the case of fire exposure, the material properties are non-smooth non-continuous functions.

As shown in Figure 8, there are five modes of failure. A Mode 1 failure, shown in Figue 8a, occurs when two criteria are met. First, the force that gypsum can resist is lower than the force resisted by the wood. Second, the moment generated by the maximum possible force applied to the gypsum is less then the moment the nail and wood can resist. For Mode 1a (Figure 8b), a similar situation arises, but instead of the gypsum failing, the wood fails. First, the force wood can resist is lower then the force resisted by gypsum. Second, when the moment generated by the maximum possible force applied to the wood is less than the moment the nail and gypsum can resist. Mode 2 failure, given in Figure 8c, occurs when the resisting moments for both the wood and gypsum are less than the moment resisted by the nail. The pivotal point can be anywhere along the nail. Figure 8d shows Mode 3, which occurs when the yield

Figure 8. Modes of Failure for Nailed Gypsum-To-Wood Connections: a) Failure of Side Member, b) Failure of Main Member, c) Failure of Side and Main Members, d) Nail Distortion and Failure of Both Side and Main Members, and e) Nail Distortion with Failure of Side Member

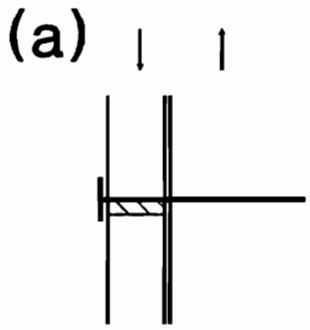

FG < FW
BMW > BMG < YM

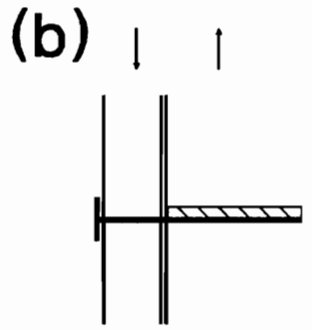

FW < FG
YM > BMW < BMG

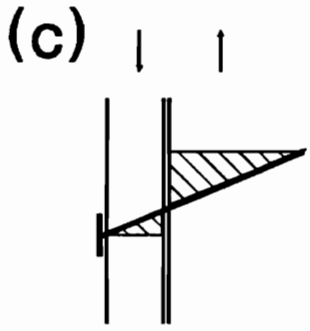

BMX = YM > RM

W - Wood
G - Gypsum
F - Embedment Force
X - Point Where the Bending Moment Equals the Yielding Moment
YM - Yielding Moment of the Nail
BM - Bending Moment Generated by the member
RM - Resisting Moment

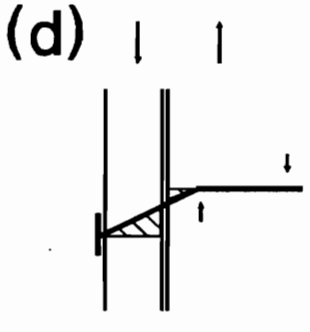

BMGW > YM < RM

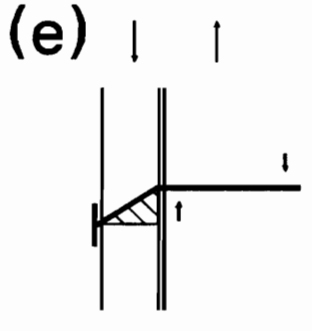

BMG > YM < RM

Figure 8.

moment of the nail is less than the generated moment and the moment the wood can resist. Mode 3a, which is shown in Figure 8e, differs from Mode 3 in that the yield moment of the nail is exceeded at a point within the gypsum. Mode 3a requires the yield moment of the nail to be less than the moment generated by the forces in the gypsum and the resisting moment in the wood.

III. COMPRESSION STIFFNESS AND STRENGTH OF GYPSUM BOARD AT ELEVATED TEMPERATURES

Introduction

The lateral loads and racking due to wind loads and earthquakes, create shear forces in structural systems. Nailed gypsum-to-stud joints add resistance to these shear forces. While the joint performance is widely documented at room temperature (Polensek 1977, 1978; Patton-Mallory and McCutcheon 1987), the performance is unknown at elevated temperatures such as those found during exposure to fire. At room temperature, the joint performance may be dictated by the compressive strength of the main or side member or by the yield strength of the nail fastener. In order to evaluate the joint performance at elevated temperatures, the high temperature properties, strength and stiffness, of the constituent materials are needed. For gypsum board, these data are not available in the literature.

This study presents the research of the compressive properties of gypsum as it is exposed to elevated temperatures. Ultimately this information will be used in an analysis that includes temperature distribution to determine whether or not a designed structure provides the expected performance at elevated temperatures such as that encountered under fire load. Compressive strength and

stiffness at discrete temperatures in the range of 50 to 140 C were investigated.

Background Information

Gypsum is calcium sulfate in combination with water ($CaSO4 \cdot 2H_2O$) in a orthorhombic crystalline structure (Windholz 1977). Gypsum board, a generic product composed principally of gypsum and covered with either paper or vinyl, is widely used as a construction material. The thickness of the materials covering the gypsum is small and causes the overall product to have a small net heat output when burned. Because of this, gypsum board has been considered a good fire barrier.

Gypsum is hygroscopic and therefore gains and loses moisture depending on the surrounding environmental conditions (Gammon 1987). The hydration or dehydration reaction is dependent on partial pressures for water vapor inside the gypsum and the surrounding materials. The crystalline structure losses water to form plaster of paris ($CaSO_4 \cdot 1/2H_2O$) between 100 C and 150 C. Within this range the reaction is called calcination. At 650 C, gypsum dehydrates into an insoluble form (Windholz 1977). In addition, the mechanical properties will change within the calcination range.

Gypsum board can also be produced with glass fibers which enables the board to retain some mechanical integrity beyond the point of calcination. The generic name for the reinforced gypsum

board is Type-X. The Uniform Building Code (UBC 1988) requires Type-X only on common walls between two different dwellings in the same building and on fire walls in a furnace room. These two situations are less common when considering all of the walls in most light-frame structures. Since Type-X walls are the exception, we have concentrated on regular gypsum in this study.

During an exposure to the standard fire curve, E-119 defined in ASTM (1989), the temperature increases very quickly in the early stages of the test. At these elevated temperatures, the nail joint that will ultimately be evaluated does not have the same ease of moisture loss along the full length. Therefore, within this test, the time of preheat and test is critical so that the minimum amount of moisture is lost and more closely resemble the actual behavior of the moisture.

Methods and Materials

The material tested was a regular 12.7 mm gypsum board product which was available at a local lumber yard. The precise composition of the panel was unknown. Each specimen was 139.7 mm long by 38.1 mm wide, and all specimens were oriented parallel to the long axis of the panel. Pretesting of rectangular specimens showed a strong tendency for end crushing. Therefore, a dog bone shape was adopted, which narrowed to 19 mm for 63.5 mm in length. This geometry was selected so that the failure would occur in the midlength and not at

the ends. Forty-two specimens were cut from one board. Specimen geometry is illustrated in Figure 9.

All of the paper was removed from each specimen to insure that the strength and stiffness were for gypsum and not for a reinforced product. The necked portions were generally free of visible defects, but some specimens contained voids, the location and size of which were recorded.

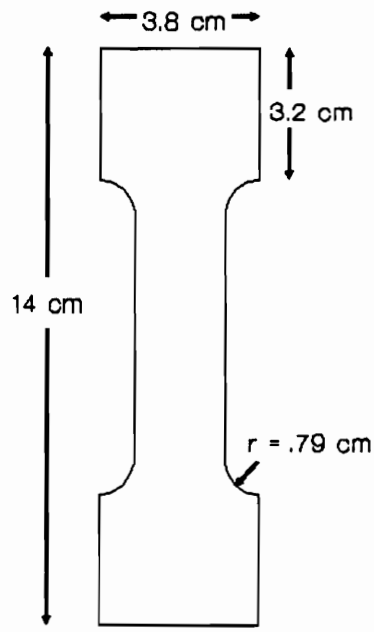

Figure 9. Diagram of the Gypsum-Board Compression Sample

Inasmuch as gypsum loses moisture of calcination at 100 C, finding the exact moisture content above the dihydrate state was difficult. The approximate moisture content was calculated by first causing the gypsum to lose all moisture above the hemihydrate state and then using the mass ratio of dihydrate state and hemihydrate state to calculate the oven-dry mass. With the oven-dry mass and the mass of the sample at equilibrium moisture condition, the actual moisture content was calculated. The samples had a moisture content above the dihydrate state of about 7%.

Mechanical tests were conducted in a temperature controlled apparatus fitted on the testing machine. The functions of the various parts of the test apparatus can be categorized as either mechanical testing or environmental control. Figure 10 shows the assembly. Restraints extending vertically 38.1 mm were attached to the compression plates on each end of the mounting fixture to reduce the tendencies to buckle and split. The compression plate columns extended through the bottom of the chamber to a load cell and through the top to the crosshead of a displacement controlled testing machine. A linear variable differential transformer (LVDT) was located on the upper extension outside the chamber. A wooden rod extended from the core of the LVDT to an arm on the lower plate in the chamber. This apparatus allowed load and displacement to be recorded without exposing the measuring devices to the high temperatures. The wooden rod was kept at a thermal steady state and

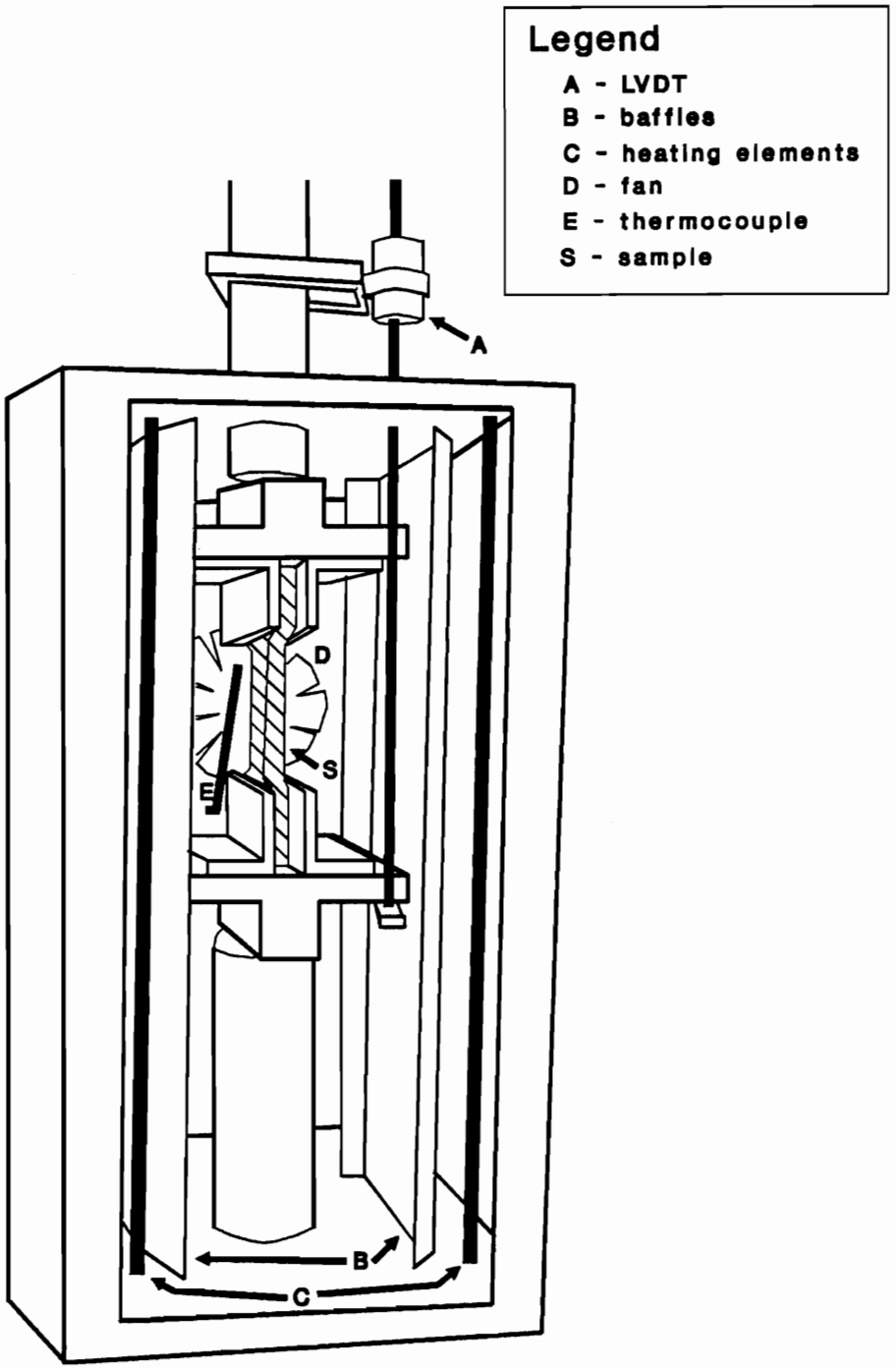

Figure 10. Schematic of the Chamber for High-Temperature Testing of Gypsum

had a low thermal expansion coefficient. These two facts insured that the displacement measurements would not be corrupted by the high temperatures.

The temperatures of the specimens were kept constant by using the thermal-environmental chamber. The temperature was held within ±1 C for all the temperatures except 50 C which was held at ±2 C. This was accomplished by placing a thermocouple in front of a fan which drew the air flow from behind the baffles where the heating elements were located to the specimen itself and back to the heating elements. The thermocouple with a Proportional / Intergral / Differential temperature controller regulated the heating elements in an on-off fashion based on the signal from the thermocouple. This was the reason for the increased temperature variation at the lower temperatures. If the voltage had been controlled, the heating elements would have heated more slowly causing the chamber to heat slower which would ultiamtely reduced the wide swing in temperature in the lower temperature range. Before any testing took place, and after each temperature change, the equipment was brought to thermal equilibrium.

The procedure for testing each specimen was broken into two time periods, preheating and actual testing. In each, the time of residence was critical. The actual factors controlling the moisture content are temperature and partial pressures. With continued heating of the air in the chamber, the partial pressures are

continually being lowered thereby increasing the drying rate. In a fire, the material near the nail joint is heated quickly with little loss of moisture. Since the mechanical properties are affected by loss of moisture, the length of time the sample is exposed to elevated temperatures is critical. In the ASTM E-119 exposure all the gypsum would reach calcination within 20 minutes.

The preheat time for a gypsum sample was calculated using published thermal values (Harmathy 1983) for a steady state conditions. The preheat time was 10 minutes.

During the testing, there were two factors to be considered. First, the amount of moisture loss was critical which required that the test be conducted rapidly. Second, the rate of testing needed to be similar to a standard so the results could be compared to other test results. The tests were conducted such that the expected time to failure was approximately 3 minutes. With this, the strain rate was 0.0118 mm/mm/min.

Temperature points for material testing were selected relative to the expected temperature of calcination. Three discrete temperature points were included before the point at which calcination would start, 50, 75, and 90 C. Four temperatures, 110, 120, 130, and 140 C, were picked within the temperature range of calcination. With these points, trends before and within the range of calcination would become apparent. Six samples were tested at each temperature.

After each test, a sketch of the failure and time to failure were recorded.

Results and Discussion

The experimental results are given in Table 2. Mean values and standard deviations are presented at each temperature investigated.

Table 2. Compression Properties of Gypsum at Discrete Elevated Temperatures

Statistic	Temperature (C)						
	50	75	90	110	120	130	140
			MOR (10^{-2} Pa)				
mean	2.795	3.34	3.529	2.403	2.491	1.657	1.383
Std.Dev.	.176	.398	.740	.174	.150	.193	.173
Δ[1]	100	120	126	86	89	59	50
			Stress at Proportional Limit(10^{-2} Pa)				
mean	2.628	3.148	3.315	2.226	2.442	1.579	1.157
Std.Dev.	.211	.738	.778	.204	.158	.189	.115
Δ[1]	100	120	126	85	93	60	44
			MOE (Pa)				
mean	6.416	8.856	11.077	5.246	3.648	2.779	1.605
Std.Dev.	1.83	3.64	4.23	1.11	.98	.64	.16
Δ[1]	100	138	173	82	57	35	25
			Strain at Failure(10^{-3} cm/cm)				
mean	5.62	8.94	5.16	6.27	7.04	9.38	11.83
Std.Dev.	1.31	7.65	2.91	1.53	.99	2.54	1.42
Δ[1]	100	159	92	112	125	167	211

1 Δ = percentage of 50 C value

As shown in Figure 11, the compressive modulus of elasticity (MOE), modulus of rupture (MOR), and stress at proportional limit showed an increase before 100 C when dehydration should have reached the dihydrate state. Then, all three compressive property values showed a decrease once the dehydration went beyond the dihydrate state where calcination occurred. This is similar to wood in that as wood dries, the mechanical properties increase. When wood becomes dry and heating is continued, it begins to degrade and loses strength and stiffness (Kollman and Côté 1968).

With strain at failure, a trend developed that was similar to MOE in effects. Below 100 C, deflection decreased causing greater stiffness. Above 100 C, deflection was greater than at 50 C and increased causing less stiffness. The two properties of stiffness, MOE and strain at failure had greater variation than did the properties of strength, MOR and stress at proportional limit. The properties of stiffness also had the most dramatic response to the temperature rises.

At lower temperatures, failure occurred more sharply at distinct points. At the higher temperatures failure tended not to occur at a distinct point of failure. Instead, there was a tendency to mash, crumble or upset. The stress reached a peak, dropped slightly and then reached a slightly higher peak. This cycle repeated itself until the ultimate stress was reached. This behavior can be considered as an elasto-pseudoplastic response. The

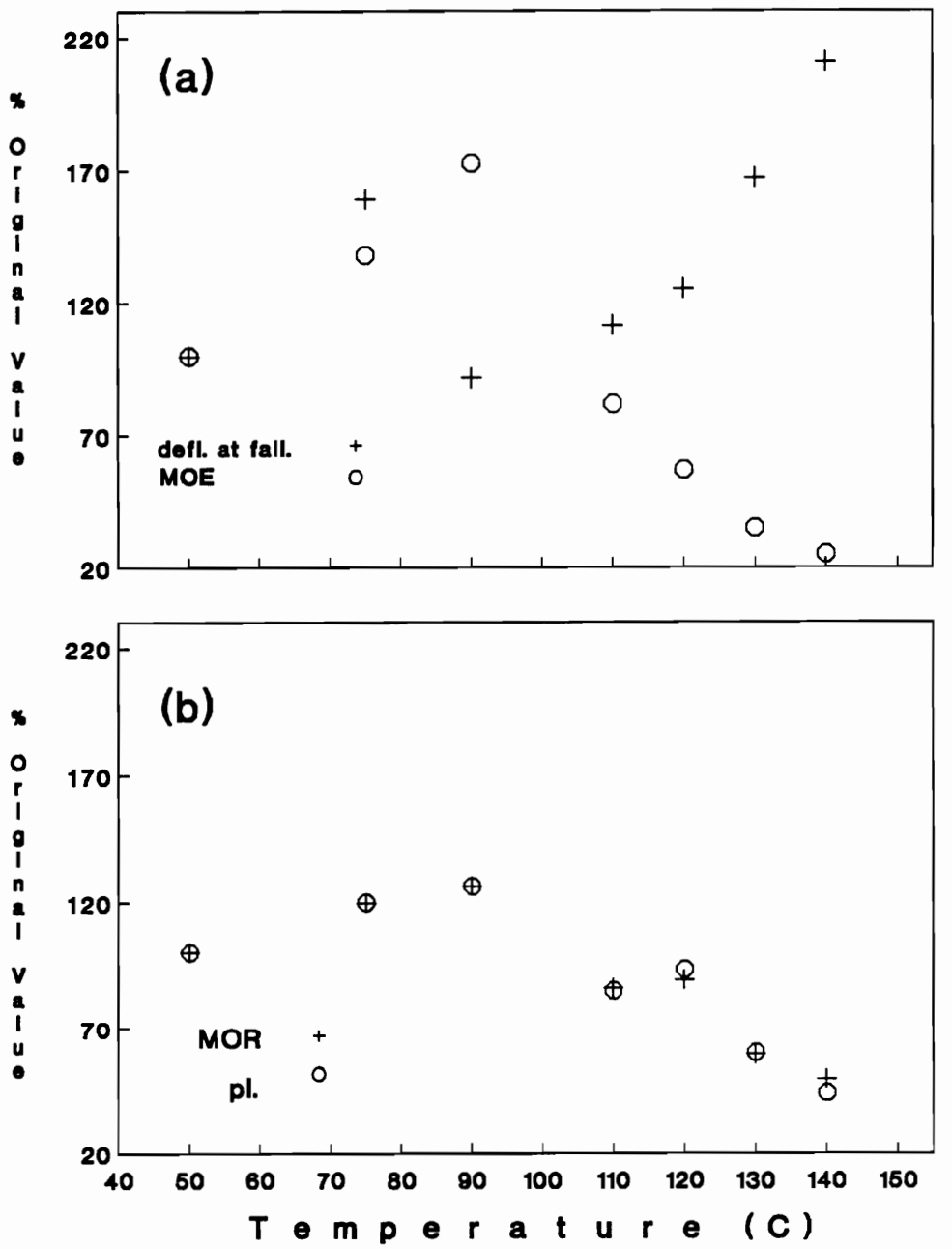

Figure 11. Effects of Temperature on the Stiffness and Strength of Gypsum Board; a) stiffness, b) strength

small increase in load at this time was reflected in the small difference between MOR and stress at proportional limit in Table 2.

In the samples with voids, failure was associated with the voids. The reasons are not clear, but the failure stresses tended to be much higher than in the samples without voids.

It is known that temperature and partial pressures affect the rate of moisture loss. However, only temperature were used for three reasons. First, temperature are easily controlled. Second, The ASTM E-119 standard fire curve only dictates the temperature of the burning gases, not heat flow nor moisture flow. Third, because the ASTM E-119 only dictates the temperature of the gases, predicting the partial pressures along the full length of the nail joint is difficult. Controlling only the temperature during the property testing will cause the most dramatic changes in the moisture content, since the partial pressures will be lower than otherwise. In this case the testing simulated the worst case scenario.

Conclusions

This study looked at the effects of temperature change on the compressive strength and stiffness of common gypsum board. The compressive properties of gypsum increased as it dried to the dihydrate form. When calcination occurred, the compressive properties were reduced quickly.

If given the temperature distribution about the joint and the properties of the constituent materials, wood, steel, and gypsum, the strength and stiffness of a nailed gypsum-to-wood stud connection could be evaluated. Depending on the temperature history of the connection, the connection could conceivably gain strength or stiffness before the ultimate loss of strength or stiffness if gypsum is the material which determined failure.

With the ability to predict the connection behavior, analysis of the wall system performance will become feasible.

IV. TEMPERATURE DISTRIBUTION ALONG A NAILED GYPSUM-TO-WOOD STUD CONNECTION AS EXPOSED TO FIRE

Introduction

As part of a structural system, the stud wall with gypsum sheathing helps resist in-plane buckling and racking. The stud-wall performance is largely dependent on the nailed connections between the sheathing and the framing members. Performance characteristics of the nailed connection has been documented at room temperature (Polensek 1977, 1978; Patton-Mallory and McCutcheon 1987). However, if the structure is subject to an intense thermal exposure such as that due to fire, the performance of the connection is unknown. To what extent the connection changes during exposure to elevated temperatures is a question that is of interest.

To determine connection performance under elevated temperatures information is needed about the mechanical properties and the temperature distribution along the nail which joins the gypsum panel to the stud. The mechanical properties of the two materials, steel and wood as a function of temperature are known (Boyes and Gall 1985, and Schaffer 1973). This study is concerned with finding the temperatures along the nail as a function of time using the finite element method. Test results of nailed gypsum-stud joints exposed to ASTM E-119 were used to confirm the finite element

results. Using finite element analysis, five cases were examined to determine the effects of the species of wood, type of gypsum board, and size of nail on the temperature distribution around the connection. Sample wall sections with embedded thermocouples were tested at the Forest Products Laboratory in Madison, Wisconsin to verify computations.

Methods

This study involved two areas of work. The first was analytical using a finite element model. The second area was an experimental investigation which involved exposing four samples to a standard fire test to confirm the results of the analytical procedure.

Computational Procedure

Five cases were examined to determine what effects three variables had on the temperature distribution. These cases with the variables are listed in Table 3.

The first case excluded the nail so that comparison with the results already published (Gammon 1987) could be made and to determine if the nail had a greater effect than the gypsum-stud interface. The stud was Douglas-fir (DF) and the sheathing was 12.7 mm regular gypsum.

Table 3. Five Analytical Cases and Variables

Case	Wood Type	Gypsum Type	Nail Size
1	Douglas-fir	regular	none
2	Douglas-fir	regular	5d[1]
3	Douglas-fir	regular	4d
4	Douglas-fir	type-X	5d
5	Spruce-Pine-Fir	regular	5d

1. d = penny weight designation

The second case included a 5 penny (5d) nail, Douglas-fir (DF), and 12.7 mm regular gypsum. This case was the basis for comparison of all the succeeding cases and experimental results.

The third case used a 4d nail rather than a 5d nail, DF stud, and regular gypsum. The building code requires 5d nails, therefore, the 4d nail represents a realistic but non-conforming case. One might hypothesize that heat may be dissipated more effectively by the longer 5d nail than a 4d nail, thus leading to lower the temperature along the nail length which ultimately affects the mechanical properties enough to change the overall behavior of the connection.

The fourth case had a 5d nail, DF stud, but the sheathing was Type-X 12.7 mm gypsum rather than regular gypsum. In most situations in a light-frame structure, regular gypsum is sufficient; the Uniform Building Code (UBC 1988) requires Type-X only on walls between two different dwellings in the same building and on fire

walls in a furnace room. Type-X gypsum has a lower amount of gypsum in the core due to the added glass fibers. The glass fibers change the thermal conductivity and the equilibrium moisture content. By changing the equilibrium moisture content, the effective specific heat is changed when the temperature is below 100 C. These differences may be enough to affect the heat flow in the joint.

Case five had 5d nails and regular 12.7 mm gypsum, but a SPF stud replaced the DF stud. Depending on the region in which the structure is located, DF or SPF may be the primary types of wood available for construction. SPF and DF have different densities and thermal conductivities which may effect the amount of heat dissipated away from the connection and thereby lowering the temperature of the connection.

Cases 3, 4, and 5 were each compared to case 2 to determine the effects wood type, gypsum type, and nail size on the temperature distribution about the nail.

The finite element method used in the analytical process consisted of simultaneously solving a system of established engineering equations which mathematically defined the physical object of interest. In this case, thermal radiation and conduction equations were used. The object of interest was divided into a finite number of smaller units, called elements, with their geometry defined by the nodes at their vertexes. Each element was described by one of the equations in the system of equations of the model.

Each equation required physical properties of the constituent materials and certain other variables. For the element representing an area where radiation is involved, the properties and values required were surface area, view factor, equivalent emissivity and absorptivity, as well as the temperatures of the heat source and receiver. The element representing an area of conduction required the values of density, thermal conductivity, specific heat, and the temperatures where the heat enters the object and the surface where the heat exits the object.

The thermal properties used for the wood stud and gypsum panel were air-dry values (Harmathy 1983) adjusted to 12% moisture content for the wood and 7% for the gypsum. These values are given in Table 4. Adjustment of thermal properties was achieved by adding the specific heat of water to the apparent specific heat of the material below the temperature at which the water would vaporize. The heat of vaporization was added to the apparent specific heat of the material at the temperature at which vaporization would occur.

The ratio of density for SPF to DF was 0.822 (Bodig and Jayne 1982). However, the thermal conductivity ratio of SPF was 0.816 of the DF thermal conductivity. The longitudinal conductivity was taken as twice that of the cross grain direction for the SPF and DF. Below 100 C, the apparent specific heat was affected by the moisture content which was in turn affected by the density. Therefore, the

apparent specific heat below 100 C was adjusted to account for the reduced moisture in SPF.

Table 4. Thermal Properties of Wood, Gypsum, and Steel

	Wood(D-F 12% MC)			Gypsum(7% MC)			Steel
Temp[1]	d[2]	k_x[3]	c[4]	d	k	c	k
25	4.5	1.47	2252	6.78	2.5	1170	450
98	4.41	"	1702	6.51	"	"	430
100	"	"	2.04E5	6.51	"	"	"
103	"	1.22	6.89E4	6.48	"	1.66E5	"
115	"	1.22	1130	6.46	"	7319	"
125	"	1.47	1150	6.44	"	880	425
200	"	"	1500	6.42	1.3	"	423
300	3.6	"	1900	6.38	"	"	400
360	1.58	"	2000	6.42	"	240	"
400	1.01	"	3552	6.41	"	880	"
500	.88	"	"	6.38	"	900	"
600	.68	"	"	6.32	"	1700	"

1. temperature - (C)
2. d - density (10^{-7} kg/mm^3)
3. k - conductivity (10^{-4} W/mmC)
4. c - effective specific heat (J/kgC)

Moisture content of gypsum is difficult to obtain because it loses moisture of calcination relatively quickly starting at 100 C. Because of this, the moisture content was determined by drying the samples at 200 C to cause it to lose the moisture of calcination. Using the mass after calcination and equation [5], the oven-dry (OD) mass was determined.

The equilibrium moisture content (EMC) was then determined using equation [6]. The results were in close agreement with data recorded by Lawson (1977).

$$M_{OD} = M_{cal} * 168.2/145.2 \quad [5]$$

where

M_{OD} = oven-dry mass (g)
M_{cal} = mass after calcination (g)
168.2 = molecular mass before calcination
145.2 = molecular mass after calcinationwhere

$$EMC = (M_{EMC} - M_{OD})/M_{OD} \quad [6]$$

where

M_{EMC} = mass at EMC

For the nail, thermal properties of low carbon steel were used (Welty, Wicks, and Wilson 1984). Table 4 lists these values.

The interior surface of an exterior wall of a light-framed building was the wall of interest. In such walls, building codes require only regular gypsum. Therefore, 12.7 mm regular gypsum was assumed rather than 15.9 mm Type-X which would have provided a one-hour fire wall instead of a 0.5-hour fire wall (Lawson 1977).

The lateral exterior surface of the stud was excluded because of the possibility that it may be exposed to a direct heat source from within the wall. This situation may occur with burn-through which could happen anytime during the fire. This was achieved by

using 12.7 mm as the distance from the surface of the nail outward in the radial direction instead of half the thickness of the stud.

Analyses with 4d and 5d nails were conducted. The following dimensions were taken from the nails used in the experimental specimens. For both the 4d and 5d nails, head and shank diameters were 7.6 mm and 2.23 mm, respectively. The length of the 5d shank was 39 mm and for the 4d, 32 mm.

When developing the finite element mesh, symmetry around the longitudinal axis of the nail was used to reduce the analysis. Cylindrical coordinates and a forty-five degree section were used as shown in Figure 12. Seven 3-dimensional isoparametric thermal elements, each with eight nodes, represented the model cross-section over the entire connection length. The elements were trapezoidal in shape with the smallest elements occurring at the longitudinal axis of the nail, the line of symmetry. The first 12.7 mm of the model, which coincided with part of the nail and the gypsum, was divided into ten even layers plus one extra layer for the thickness of the nail head. The portion coinciding with rest of the nail and the wood stud was divided into seven layers of increasing length. This geometry was selected for two reasons. First, thermal effects were expected to diminish with increasing distance from the heat source. Furthermore, the total connection length was much greater than the thickness of the gypsum. Five cross section layers were added beyond the end of the nail to represent the wood beyond the nail.

The nodes corresponding to the first two elements in these last five cross section layers were shifted closer to the longitudinal axis to allow for the end of the nail to be tapered.

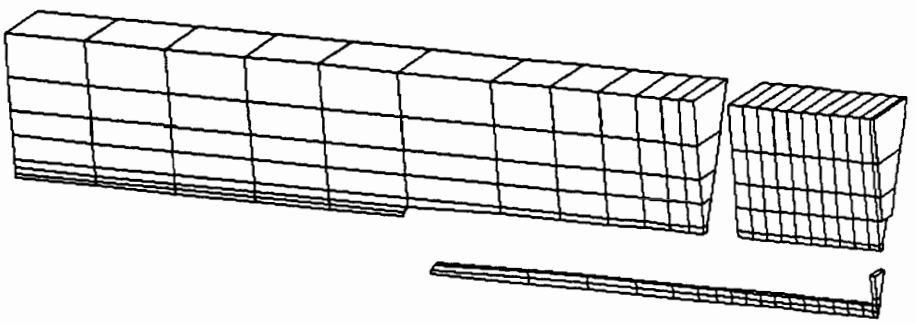

Figure 12. Finite Element Mesh for the Thermal Analysis of a Nailed Gypsum-to-Wood Connection

In a real wall there is a small space between the gypsum board and the stud. The discontinuity of the gypsum-wood interface affects the conductivity of the real wall. The model was first run with the gypsum-wood interface being in intimate contact, not having a gap between the two materials.

With a dynamic problem, temperature steps, time steps, and the number of increments within the time steps can be critical. For the

input data representing thermal load, only the temperature at the end of the time step was given. The finite element program assigned temperatures for each time increment by assuming that the time-temperature function within each time step was a linear function. The time steps must coincide with a roughly linear segment of the time-temperature curve to be used. In this study, the time-temperature curve was ASTM E-119 (1988). An approximation of the optimum time interval is given in equation [7] (Baran 1988).

$$\text{Time interval} \geq l^2/4\alpha \qquad [7]$$

where

l = conduction length of the smallest element (mm)
α = thermal diffusivity (mm^2/sec)

Using this equation to find a time interval as a start, convergence of temperatures was found at a time step of five minutes with 20 equal intervals. The input radiation constants were used to model a fire 91 cm from the wall while assuming the connection was positioned 122 cm from the floor. These values were used so as to compare the results with previously published results and to typify the average joint.

Experimental Procedure

To verify the computational results of case 2, four wall sections, 51 by 25 cm, were constructed for fire testing. As shown in Figure 13, each model had two joints to be monitored. By including two joints in each test, the consistency of the test method could be examined.

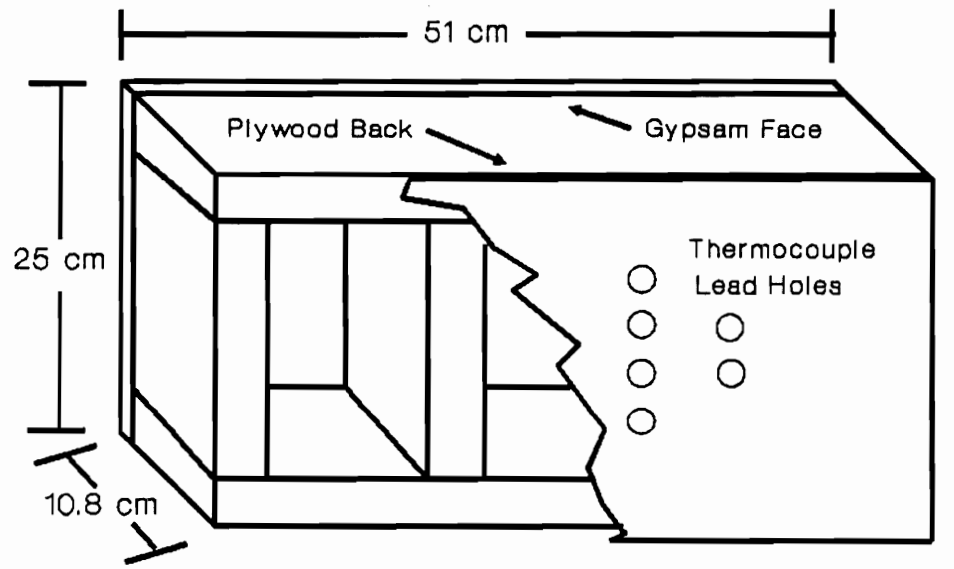

Figure 13. Diagram of Fire-Test Assembly

The wall models were constructed of 12.7 mm regular gypsum on the exposed side and 6.4 mm plywood on the unexposed side nailed to the frame with the same type of nails used in the test joints. Four 2 by 4 studs were evenly spaced across the width and one each on the top and bottom of the sample. The test joints were placed in the two central studs.

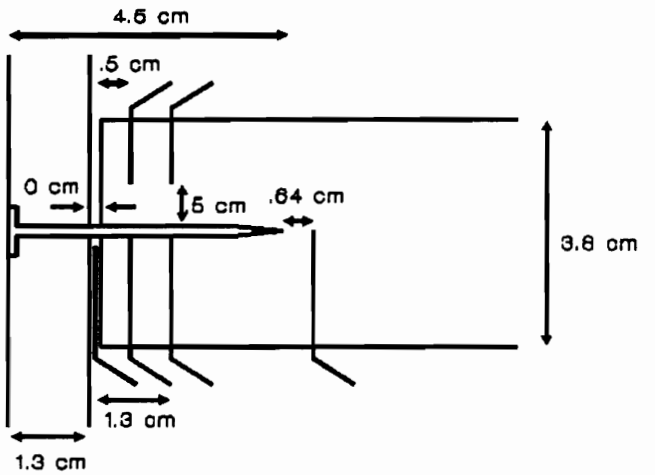

Figure 14. Thermocouple Position and Connection Configuration for Fire-Test Units

For each test joint, temperatures were recorded with thermocouples located at six points. The positions of the

thermocouple points are shown in Figure 14. Points 1 and 2 were in line in the gypsum-stud interface at 2 mm and 13 mm respectively from the nail surface. Points 3 and 4 were located on the nail at 5.1 and 12.7 mm from the gypsum-stud interface. Points 5 and 6 were 5 mm from the surface of the nail and also located 5.1 and 12.7 mm from the gypsum-wood interface. All six points coincided with nodes in the finite element analysis.

To position the thermocouples, which were made of 30-gauge Type-K thermocouple wire, a pilot hole was drilled for the nail and then the holes for the thermocouples were drilled from the side of the stud to the pilot hole. The nail was driven in after the thermocouples were in place. After the nail had been driven into position, electrical conductivity was checked to insure that physical contact was made between the nail and thermocouple and that the integrity of the thermocouple was intact.

Results and Discussion

An initial run of the analytical model was made without the nail but with the same gross geometry (case 1) in order to compare these results with previously published results which did not include a nail joint in the wall (Gammon 1987). In Gammon's study, burn-through was predicted with good results. Comparison of results showed Gammon's model yielded lower temperatures. In order for this

model and Gammon's to agree, the thermal loads had to be significantly reduced.

With this disagreement noted, the nail was added and the four remaining cases were evaluated. A comparison of case 1 with no nail and the four cases with the nail showed that the thermal conductivity of the nail caused a heat transfer of a magnitude that overshadowed any effect the gypsum-wood interface would have on the flow of heat. Because of this, the interface conductivity was left unaltered.

Figure 15 shows the temperature along the length of the nail at five-minute intervals for case 2. In the distance representing the thickness of the gypsum board, the temperature decreased rapidly away from the exposed surface. Within the wood stud, the rate of temperature decline was reduced.

Figure 16 shows the time-temperature relation from case 2 for six specific points from which coincided with the thermocouples of the joint samples exposed to the standard fire curve. Figure 16 also shows the ranges of temperatures for the thermocouples. Figures 16c and 16e represent the two points on the surface of the nail. The temperatures of the computational results were slightly higher than the experimental values. The time step 4 in Figure 16c showed the largest deviation. The difference was attributed to the thermal conductivity of the real nail which must have been lower than the value used in the analysis.

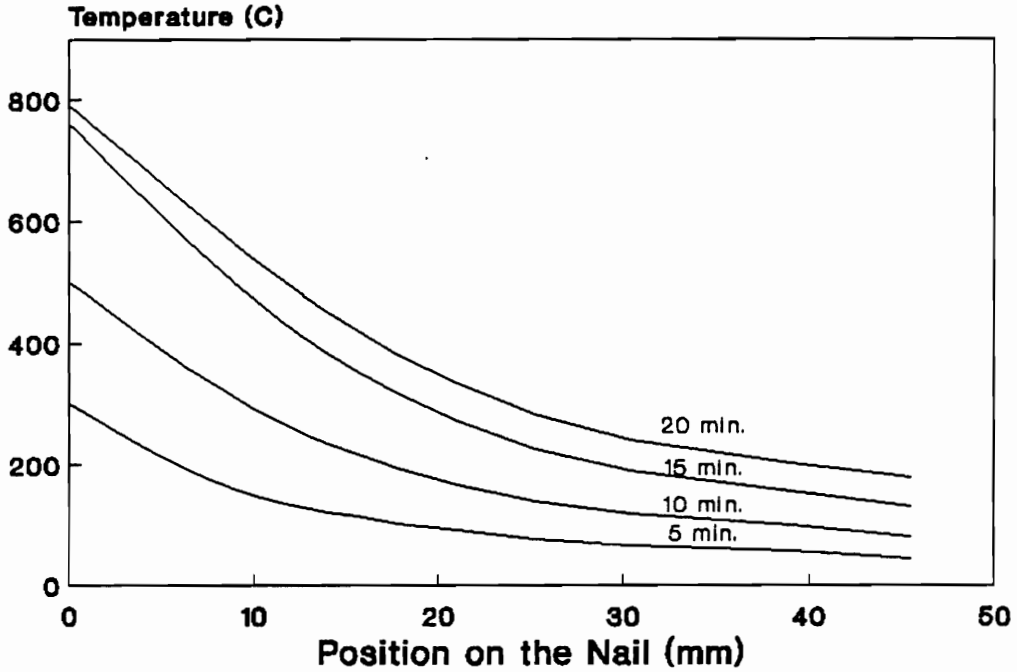

Figure 15. Computed Temperatures Along the Nail at Five-Minute Intervals

Figure 16a is only 2 mm away from the nail, and the analytical results were slightly low. The experimental results displayed a inflection at about 100 C. The inflection can be related to the moisture content effects.

Figures 16b, 16d, and 16f depict the points which were surrounded by wood or gypsum and not in contact with the nail. These Figures exhibit a dwell point at about 100 C for the numerical analysis and the experimental data. This again demonstrates the

16. High and Low Temperatures of the Test Joint Thermocouples (+) and Temperatures From the Finite Element Model Corresponding Points (-): a) 2 mm From the Nail in the Interface, b) 13 mm From the Nail in the Interface, c) on the Nail, 5.1 mm From the Interface, d) 5 mm From the Nail, 5.1 mm From the Interface, e) on the Nail, 12.7 mm From the Interface, and f) 5 mm From the Nail, 12.7 mm From the Interface

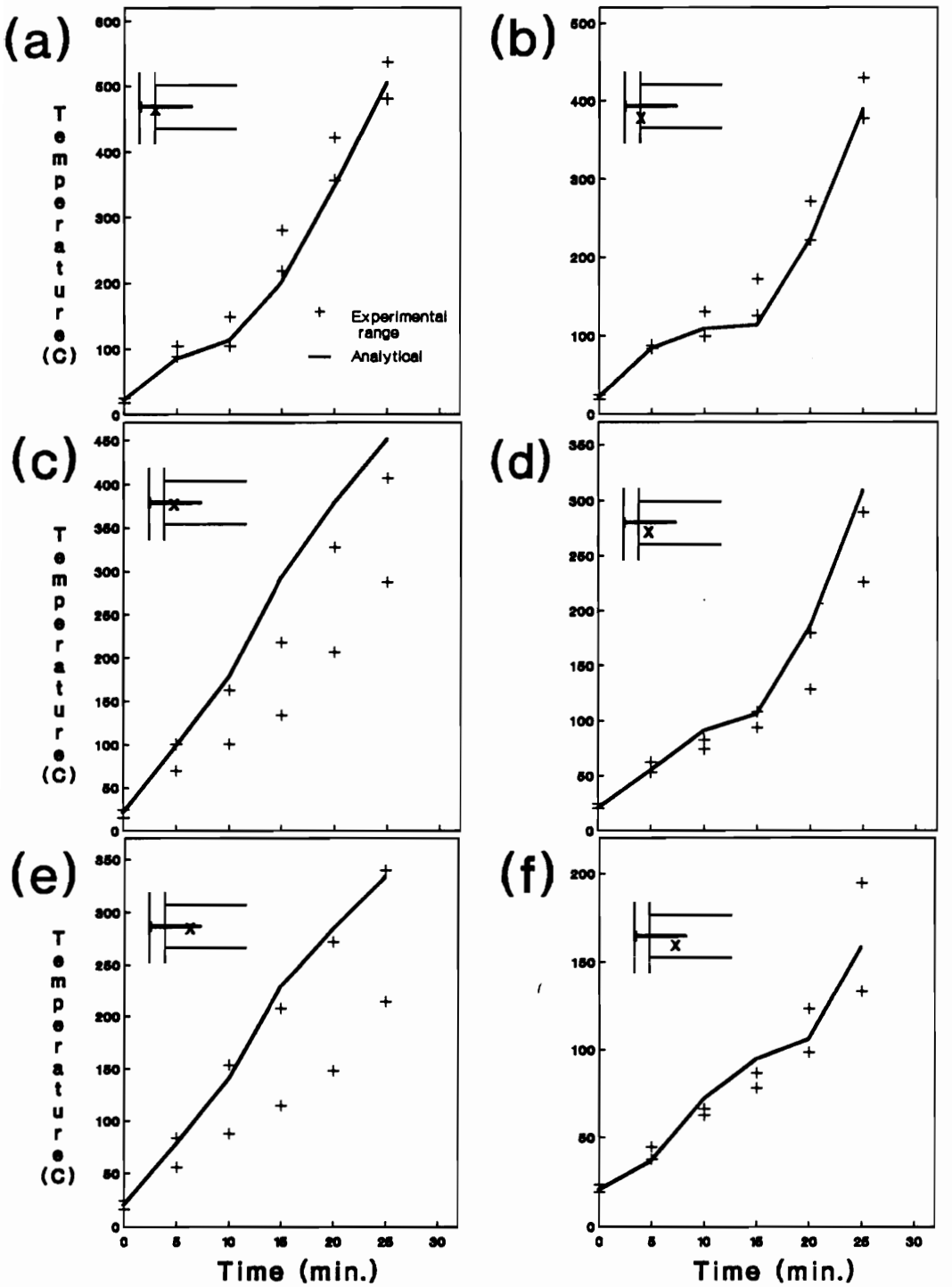
(a)
(b)
(c)
(d)
(e)
(f)
Temperature (C)
Experimental range
Analytical
Time (min.)

Figure 16.

effect that the moisture content has on the temperature. In Figures 16d and 16f, the high moisture-content front can be followed by the dwell points at 100 C. In general, there was good agreement between the analytical and experimental data.

In this study, the main regions of interest in the model were the nail and the material adjacent to the nail. Cases 2 and 3 showed that within these regions, no significant differences in the temperatures occurred when the nail size was decreased from 5d to 4d. These results are supported by Chinniah (1989). Chinniah reported that the depth of char along the nail was constant regardless of the nail length. He also found the temperatures along the nail to follow the same function regardless of nail length. In this study, the greatest temperature difference attributed to nail size was at the tip of the nail at the end of step six in the model; results from the 4d model were 8 C lower.

Effect of wood type, DF as opposed to SPF, was examined by contrasting cases 2 and 5. The greatest temperature difference was 18 C higher in the SPF case at the end of step six. In the model of the nail, this occurred 2.8 cm from the exposed surface.

The type of gypsum board, regular or Type-X, was considered by cases 2 and 4. Here, the greatest temperature difference was an 18 C increase in the Type-X gypsum at the end of step six. In the model, this occurred on the nail 1 cm from the exposed surface of the wall.

In a study of nailed connection performance by Chou (1987), a gap was assumed to exist between the gypsum and the wood stud. The gap development was based on shrinkage of the green stud as it dried. However, a finite element model with a gap was not developed for this study. Analysis including the gap was not deemed necessary because the temperatures that were of interest were those in the nail and in the material immediately adjacent to the nail. The bulk of the heat flow to these areas was through the nail. If the gap was included it would act as an insulator, decreasing the amount of heat flow to the material immediately adjacent to the nail by avenues other than through the nail. If in future studies, the gap was to be included, three dimensional conduction elements could be inserted between the wood and the gypsum with the appropriate thermal conductive value.

Conclusion

In this study, the ability to predict the temperatures within a nailed gypsum-to-stud connection as exposed to elevated temperatures has been demonstrated. It reconfirms the effect that moisture content has on the temperature of hydroscopic materials and therefore the effects on the mechanical properties at elevated temperatures.

The results showed that neither the wood type, nail size, or type of gypsum board significantly affected the temperature

distribution along the connection. This data provides valuable information needed to evaluate the mechanical behavior of such connections under fire load. Because the materials do not affect the temperature distribution, the mechanical properties resulting from the temperature distribution will determine the performance of the connection. With this system, designers and code developers can determine the specifications the connection requirements under fire

V. THE THERMO-MECHANICAL PERFORMANCE OF THE CONNECTION

Introduction

Studies of nailed sheathing-to-stud connections are numerous (Polensek 1977, 1978; Patton-Mallory and McCutcheon 1987) but do not include gypsum as a sheathing material during an exposure to fire. Under normal circumstances, one of the main functions of the gypsum board is to provide a substrate for decorative materials. However, gypsum board also provides strength to the frame of the structure to resist racking and lateral loads (Oliva and Wolfe 1988) as well as a thermal barrier to the framing materials during a fire.

The fire resistance of gypsum board, or thermal protection to the frame of a structure, is well documented (Gypsum Association 1988). However, the strength it provides during a fire exposure has not been studied. Before the thermo-mechanical behavior of a connection which resists lateral loads can be evaluated, the temperature distribution along the connection and the thermal-dependent mechanical properties of the constituent materials are needed. This information was accumulated in two previous studies (Chapter III, Chapter IV).

With results of Chapters III and IV, this study used an extension of the yield theory of connections by Aune and Patton-Mallory (1986a). This study will determine the strength and mode of

failure of the connection for the first 25 minutes of exposure with ASTM E-119 (1988) as the thermal load. With these results, the strength of the connection that resists racking and lateral loads on the wall systems of a light-frame structure can be predicted. Structural design professionals will then have the ability to determine whether or not the structure provides the expected performance during the fire.

Background

Nailed connections typically have been examined using foundation modulus (Wilkinson 1971). With constant material properties, the equations are reasonable. However, when the material properties along the length of the connection are not smooth, constant functions, the problem of solving the equations is greatly increased. A nailed gypsum-to-stud connection provides such a situation. Möller (1950) used the yield theory which assumed all materials exhibited ideal plastic behavior to explain failure of nailed connections (Aune and Patton-Mallory 1986). Ideal plastic response is when deformation does not occur until a level of stress is reached such that additional deformation requires no additional stress.

Depending on the materials and geometry, various modes of failure are possible. The five modes of failure considered here are shown in Figure 8 with the associated governing conditions. The

governing conditions are based on comparing the yield moment for the nail to the moment that is generated by the side and main members which are restricted by the crushing stress they can resist, i.e. the material embedment strengths. With the types of structural failures that are of concern here, i.e. racking and in-plane buckling, once displacement starts the load which the structure is able to resist drops off sharply. Since the yield theory predicts a load at which displacement starts to occur, this method predicts the maximum loading situation.

Using the yield theory method requires that the materials fulfill the assumption of ideal plastic behavior. Steel being elasto-plastic comes very close to exhibiting ideal plastic behavior and wood was shown to adequately satisfy this assumption (Aune and Patton-Mallory 1986a). While these materials continue to display plastic behavior at elevated temperatures the magnitude of yield strength decreases. The yield stress of low carbon steel as a function of temperature is depicted in Figure 6 (Boyes and Gall 1985).

No published data was found for embedment strength of wood during exposure to fire loads. The relationship of temperature and compressive strength of wood parallel to grain is shown in Figure 5 (Schaffer 1973). Above 290 C, wood is reduced to char and has little strength. Because of the char development, the embedment strength above 290 C was considered to be zero for this study.

In some situations, the direction of the force on a laterally loaded nail connection applied is perpendicular to grain. At room temperature, Hunt and Bryant (1990) reports the embedment strength perpendicular to grain is between 67% and 220% that of parallel to grain. Chinniah (1989) reports that nailed steel gusset plates loaded parallel to grain behaved in an elasto-plastic manner. He also reported that the same connection type loaded perpendicular to grain behaved less plastically and a had a higher ultimate load. This data suggested that the embedment strength of wood perpendicular and parallel to grain could be the same curve as compressive strength parallel to the grain but with a different y intercept.

For gypsum board, the strength and stiffness at elevated temperatures were gathered in a recent study (Chapter III). The compressive strength of gypsum board is depicted in Figure 11b. The study indicated that gypsum board is an elasto-pseuoplastic material. The results also showed gypsum board increased in compressive strength as the temperature approached 100 C, where calcination starts. This increase in strength was hypothesized to be caused by the loss of moisture above the dihydrate state of gypsum. After 100 C the strength sharply decreased. Again this was hypothesized to be the result of the composition of gypsum progressing from the dihydrate state to a hemihydrate state. The structure of gypsum does not change in the temperature range of 150

C to 360 C. Considering this data, the strength was assumed to be constant if the temperature was less than 360 C and then was assumed to be zero at temperatures over 360 C.

In a second study (Chapter IV), the temperature distribution along a nailed gypsum-to-wood stud connection was determined using the standard fire curve, ASTM E-119 (1988), as the thermal load. The analysis was achieved by using the finite element method. Confirmation of the results was acquired by subjecting four specimens to the furnace test as outlined in ASTM E-119. There was good agreement between the calculated temperatures and experimental results. By extending the finite element analysis, a series of evaluations included an examination of the effects on temperature distribution as caused by species of wood in the stud, regular gypsum board versus Type-X gypsum board, and nail characteristics. It was found that none of these variables had any significant effects on the temperature distribution about the nailed connection.

Methods

Single equations can be derived for each mode of failure for the yield theory if the material properties are constant. With the material properties varying in a non-smooth and non-continuous fashion, another approach was sought. The approach used here to determine the connection behavior was to compare the possible

moments and forces along the connection. A systematic method was needed to provide an efficient routine.

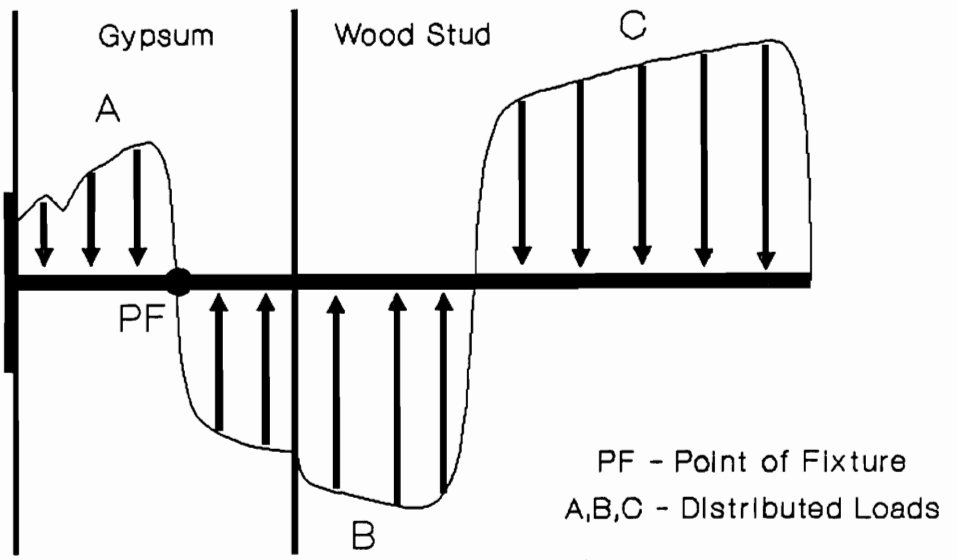

Figure 17. Diagram of a Nailed Gypsum-To-Stud Connection With Distributed Loads

Before describing the method used in determining the possible moments and forces, a few definitions are needed. Refer to Figure 17. The first definition, point of fixture on the cantilever beam, is where an imaginary clamp is positioned. The imaginary clamp represents the foundation, which has rigid and fixed boundary conditions. The second definition, yield moment, was considered as

the moment at which yield in the nail was initiated. Bending moment refers to the bending moment generated in the cantilever beam by the distributed load A about the point of fixture. The final definition, the resisting moment, was the moment that the foundation could resist and was composed of two distributed loads of opposite directions and over the length between the point of fixture and the end of the nail so that the net force of A, B, and C was zero.

The flow chart in Figure 18 shows the process for the analysis of the connection performance. Initially, a temperature distribution file was established for various points along the connection at set time increments during a fire. A second file was established containing mechanical property responses to elevated temperatures of the constituent materials. These two files, as listed in Appendix A, were utilized in a cubic spline computer program to establish a file composed of the mechanical properties along the connection at the set time intervals. This final file was employed in the connection behavior computer program.

The initial step in the connection behavior computer program was the calculation of the forces that the wood and gypsum could withstand before yield occurred and the bending moment generated by the distributed loads from the embedment forces. The possibility of a point of fixture, shown in Figure 17, at which the bending moment equaled the yield moment of the nail was next determined. To find the point at which the bending moment equaled the yield moment, the

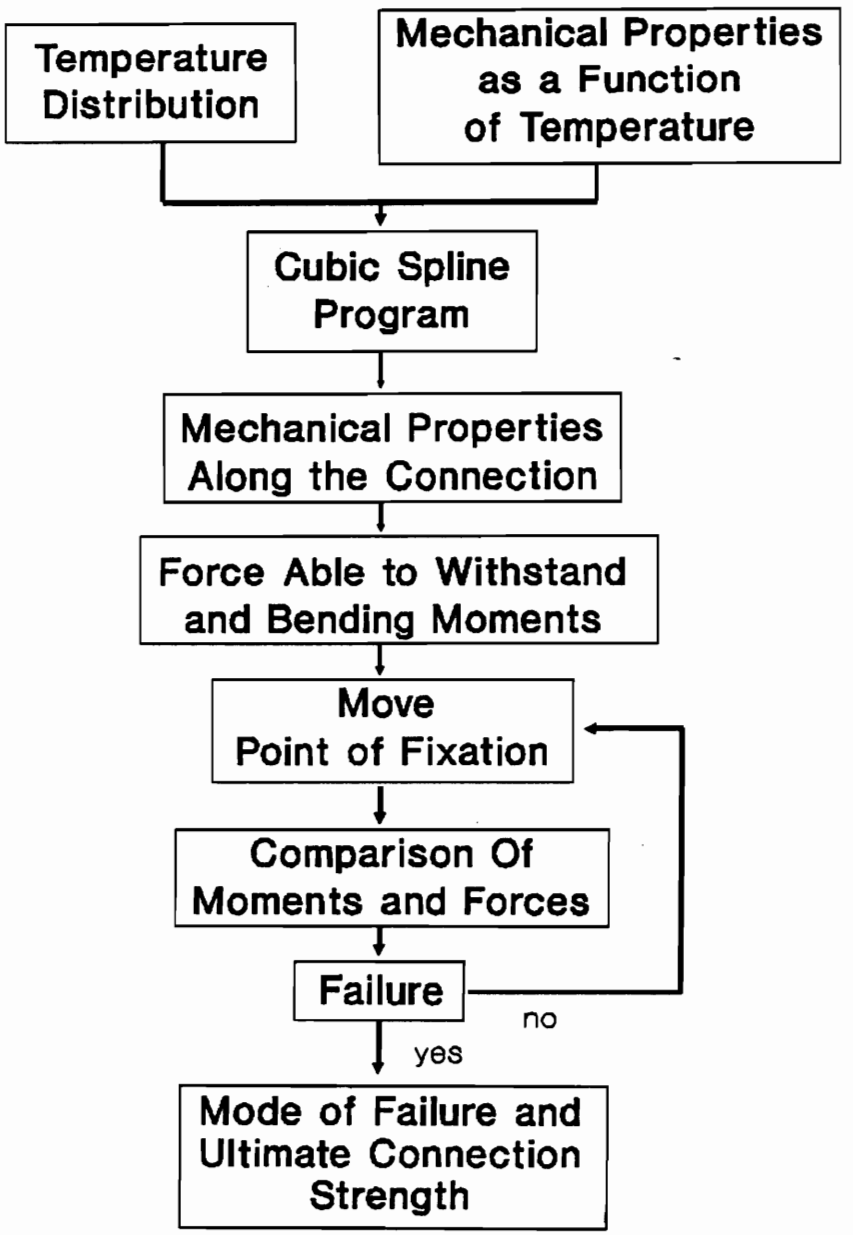

Figure 18. Flow Chart Used to Determine the Strength of a Nailed Gypsum-To-Stud Connection

bending moment was calculated each time the point of fixture was moved successively along the nail away from the surface of the wall. When the generated moment exceeded the yield moment, interpolation was carried out until they were equal. If there was such a point, the resisting moment was found. To find the resisting moment, the point at which the distributed load changed direction was found, producing a net force of zero, and the moment was calculated. At this time, the forces and moments were examined to determine which mode of failure would occur and the force that the joint could withstand.

Results and Discussion

In this study, it was of interest to see what effect wood species, direction of force, and nail length had on the total strength of the joint as well as the effects a fire had as the thermal load. Of all these variables, only thermal load had any effect on the ultimate strength of the connection. The minor temperature changes caused by the material changes being investigated did not effect the mode of failure or the ultimate strength. The difference in wood strength when the grain direction was changed from parallel to grain to perpendicular to grain had no effect on the strength of the connection. The limiting factor in the connection was the strength of the gypsum. The connection failure was always a mode 1 failure. Table 5 shows the mode of

failure and the failure load in increments of five minutes. An increase in ultimate strength was observed in the first five minutes of exposure. The temperature of the gypsum board is below 360 C, before the destruction of the hemihydrate state is initiated. The inside surface of the gypsum board is below 100 C corresponding to the initiation of the destruction of dihydrate state into the hemihydrate state. The strength then sharply decreased corresponding to the continued loss of moisture with the rapid rise in temperature.

Table 5. The Strength and Mode of Failure With Corresponding Temperatures for a Nailed Gypsum-To-Stud Connection at Five-Minute Intervals When Exposed to Fire in the Model

Time (min.)	Temperature (C)			Mode of Failure	Strength (N)
	Fire	Nail Head	Stud Surface		
0	20	20	20	1	28.1
5	538	294	92	1	29.3
10	704	493	153	1	16.1
15	760	751	265	1	11.3
20	795	782	374	1	11.8
25	821	793	472	1	6.4

Conclusion

Within this study the nailed gypsum-to-stud connection of a light-frame structure was examined to determine the effects of fire load on the mode of failure and the strength. Failure load and mode was determined during the first 25 minutes of fire exposure by using the yield theory for connections. Embedment strength of the gypsum board was critical to connection performance. During the first five minutes, the strength of the connection increased due to the moisture loss from the gypsum board before the onset of calcination. The connection strength after this time decreased due to the start of calcination in the gypsum board. The variables, i.e. stud material (species and grain orientation), gypsum board type, and nail size had no effect on the strength of the connection.

Knowing that the embedment strength of gypsum board determines the strength of the connection, building codes could conceivably be changed to allow smaller size nails for attaching the gypsum board to the stud thereby reducing the cost of construction and occurrence of nail popping. Using this model, designers are now able to predict the strength of the gypsum-to-wood stud connection under fire load in a light-frame structure.

VI. SUMMARY

The behavior of nailed connections under laterial loading has been extensively studied. The lack of incorporating a fire load has hindered the evaluation of racking strength of walls during a fire. A mechancial behavior analysis was performed on the gypsum to wood stud nailed joint as exposed to fire.

The first step was to accumulate the mechanical properties of the materials in the joint, i.e. wood, steel, and gypsum as it relates to temperature. The wood and steel material properties were obtained in the literature. The mechanical properties for gypsum were data from actual experimentation. Gypsum was found to increase in compressive strength as the moisture content approached the dihydrate state and to then decrease sharply in compressive strength as the moisture content approached the hemihydrate state. Gypsum also had a pseudo-plastic behavior as it approaches maximum strength in the form of crushing. This behavior was more pronounced as the moisture content approaches the hemihydrate state.

The next step was to accumulate the temperature distribution along the nail at set increments of time. This was approached analytically, using a finite element model, and confirmed experimentally. The analytical results were in close agreement with the ranges obtained experimentally. The analytical results showed that the temperature did not change appreciably with changes in stud species, nail length, or gypsum type.

The final step was to incorporate the two previous results and develope an analytical model to predict the strength of the joint at set time intervals during fire exposure using the yield theory. With this model, the strength of gypsum was found to be the determining factor in the joints strength. Both the nail and the wood were significantly stronger so as not to determine the failure strength. The orientation of the laterial loading with respect to grain direction of the stud did not effect the strength of the connection.

With these results for a single connection, prediction of the racking strength of an entire wall can be determine by expanding the data in order to acccount for connections spread over the wall from the floor to the ceiling. Accumulating this data could be accomplished by changing the view factor in the radiation heat flow equation. The view factor in this study was assumed a height 1.2 m for the connection. The height would vary from zero to 2.4 m.

Further studies could involve fire intensity and fire growth. Inasmuch as an initiating fire is not global in terms of a building and may fires are not as intense as the standard ASTM E-119 fire, the strength of the connection would not deteriorate as rapidly. The racking strength of the wall would therfore be greater. Data for connections exposed to various fire conditions could be accumulated by changing the view factor, distance from the fire, and gas temperature while using the procedures followed in this study. This

expanded data could assist in predicting racking strength of walls subjected to a full range of exposure.

Sheathing, being a main component of the connection, if changed could effect the net behavior of the connection. Type-X and regular gypsum thicker than 12.7mm would increase the strength of the connection. Wood composites may delaminate at elevated temperatures and the insulating effects are thereby reduced. The degradation of the wood composites may out weigh the higher embedment strength they offer. Additional studies are needed to determine the net effects.

These further studies would more quickly bring about the ultimate purpose of a design professional, to design a structure that meets safety and serviceability criteria.

BIBLIOGRAPHY

American Soiety for Testing and Materials. 1988. Annual Book of ASTM Standard. vol 04.07. Philadelphia, PA. 943pp.

Aune,P., and M. Patton-Mallory. 1986. Lateral load-bearing capacity of nailed joints based on the yield theory - theoretical development. Res. pap. 469 USDA Forest Service, Forest Products Lab, Madison, WI.

_____, and _____. 1986. Lateral load-bearing capacity of nailed joints based on the yield theory - experimental verification. Res. pap. 470 USDA Forest Service, Forest Products Lab, Madison, WI.

Avent, R., and C. Issa. 1984. Effect of fire on epoxy-repaired timber. Journal of Structural Engineering. 10(12):2858-2878.

Baran, N. 1988. Finite Element Analysis on Microcomputers. McGraw-Hill Book Company. New York, N.Y. 219-231 pp.

Beall, F. 1972. Introduction to thermal analysis in the combustion of wood. Wood Science. 5(2):102-108.

Beall, F., and H. Eickner. 1970. Thermal degradation of wood components: a review of the literature. Res. pap. 130 USDA Forest Service, Forest Products Lab, Madison, WI. 26pp.

Berkowitz, N. 1957. The differential thermal analysis of coal. Fuel 36:355-373

Blackshear, P., and K. Murty. 1965. Heat and mass transfer to, from and within cellulosic solids burning in air. Pages 911-923 in 10th symposium international combustion. The Combustion Institute, Pittsburgh, PA.

Bodig, J., and B. A. Jayne. 1982. Mechanics of Wood and Wood Composites. Van Nostrand Reinhold Company. New York, N.Y.

Boyes, H., and T. Gall. 1985. Metals Handbook desk edition. American Society of Metals.

Chang, F. 1986a. Stress analysis of wooden structures exposed to elevated temperatures. Journal of Reinforced Plastics and Composites. 5:218-238.

_____. 1986. Thermal-mechanical loading interaction effect on strength and failure time of wooden structures exposed to elevated temperature. Journal of Reinforced Plastics and Composites. 5:253-271.

Chinniah, R., 1989. Fire performance of nailed gusset connections between glulam members. M.S. Thesis. University of Canterbury, Christchurch, New Zealand. 126pp.

Chou, C. 1987. Modeling of nonlinear stiffness and nonviscous damping in nailed joints between wood and plywood. Ph.D. dissertation, Oregon State University, Corvallis, OR. 181pp.

Gammon, B. 1987. Reliability analysis of wood frame wall assemblies exposed to fire. Ph.D. dissertation, University of California Berkley, CA. 377pp.

Goring, D. 1963. Thermal softening of lignin, hemicellulose and cellulose. Pulp and Paper of Canada. 64(12):t517-t527.

Gypsum Association. 1988. Fire resistance and sound control design manual. Chicago, IL.

Harmathy, T. 1983. Properties of building materials at elevated temperatures. National Research Council of Canada Div. of Building Research. DBR no. 1080 Ottawa. 77pp.

Hetenyi, M. 1946. Beams on Elastic Foundation: Theory with Applications in the Fields of Civil and Mechanical Engineering. University of Michigan Scientific Series vol. xvi. The University Press Michigan. Ann Arbor, Mich. 255pp.

Hunt, R., and A. Bryant. 1990. Laterally loaded nail joints in wood. Journal of Structural Engineering. 116(1):111-124.

International Conference of Building Officials. 1988. Uniform Building Code. Whitter, California.

Jeanes, D. 1985. Computer modeling the fire endurance of floor systems in steel-framed buildings. Fire Saftey: Science and Engineering. ASTM STP 882, T.Z. Harmathy, Ed., American Society for Testing and Materials. Philadelphia, PA. 223-238 pp.

Kansa, E., H. Perlee, and R. Chaiken. 1977. Math model of wood pyrolysis including internal forced convection. Combustion and Flame. 29(3):311-324.

Kanury, M., and P. Blackshear. 1970a. Mass regression in the pyrolysis of pine wood macrocylinder. Combustion Scienc and Technolgy. 9:31-36.

_____, and _____. 1970b. Some consideration pertaining to the problem of wood burning. Combustion Science and Technology. 1:339-355.

Kanury, M. 1972a. Burning rate of wood. Combustion Science and Technology. 5:135-146.

_____. 1972b. Thermal decomposition kinetics of wood pyrolysis. Combustion and Flame. 18(1):75-83.

_____. 1973. Rate of charring combustion in a fire. Pages 1131-1142 in 14th International Symposium on Combustion. Combustion Institute, Pittsburgh, PA.

Kollman, F., and W. Cote. 1968. Principles of Wood Science and Technology Vol. I. Solid Wood. Springer-Verlag New York Inc pg 310.

Kuenzi, E. 1953. Theoretical design of a nailed or bolted joint under lateral load. Res. pap. 1951 USDA Forest Service, Forest Products Lab, Madison, WI. 29pp.

Kuber, H. 1982. Heat release in thermally disintegrating wood. Wood and Fiber. 14(3):166-177.

Lawson, J. 1977. An evaluation of fire properties of generic gypsum board products. Center for Fire Research, National Bureau of Standards. Washington D.C. 22pp.

Möller,T. 1950. New method of estimating the bearing strength of nailed wood connections. No. 117 Gothenburg, Sweden:Chalmers Teniska Högskolas.

North American Wood Products Fire Research Consortium. 1989. Minutes of the Fire Modeling Subcommittee. June 6-7 1989. page 2. Modeling heat transfer through wood-stud partitions.

National Safety Council. 1989. Accident Facts. Washington, D.C. 104pp.

Oliva, M., R. Wolfe. 1988. Contributions of gypsum wallboard to racking performance of walls. Pages 759-765 in Proceeding of the 1988 International Conference on Timber Engineering, vol.1. Forest Products Research Society, Madison, WI

Patton-Mallory M., and W. McCutcheon. 1987. Predicting racking performance of walls sheathed on both sides. Forest Products Journal. 37(9):27-32.

Polensek A. 1977. Strength and stiffness of walls with wood and steel studs. Forest Product Journal. 27(2):45-53.

_____. 1978. Properties of components and joints for rational design procedure of wood stud walls. Wood Science. 10(4):167-175.

Roberts, A., and G. Clough. 1963. Thermal decomposition of wood in an inert atmosphere. Pages 158-166 in 9th Symposium on Combustion. Combustion Institute, Pittsburgh, PA.

Sano, E. 1961. Effects of temperature on mechanical properties of wood I: compression parallel-to-grain. Journal of Japan Wood Research Society. 7(4):147-150.

Schaffer, E. 1967. Charring rate of selected woods -transverse to grain. Res. pap. 69. USDA Forest Service, Forest Products Lab, Madison, WI. 21pp.

_____. 1973. Effects of pyrolytic temperature on the longitudinal strength of dry D-fir. Journal of Testing and Evaluation. 1(4):319-329.

_____. 1977. State of structural timber fire endurance. Wood and Fiber. 9(2):145-170.

Sherwood, G., and R. Moody. 1989. Light-frame wall and floor systems analysis and performance. Res. pap. GTR-59 USDA Forest Service, Forest Products Lab, Madison, WI. 162pp.

Skaar, C. 1978. Energy Requirements for drying lumber VPI&SU Pub.

Swanson Analysis Systems. 1988. Ansys PC/Thermal 4.3 Reference Manual. Houston, Pa. pp 11.1-11.35.

Welty, J., C. Wicks, and R. Wilson. 1984. Fundamentals of Momentum, Heat and Mass Transfer, 3 rd. edition John Wiley and Sons. New York, NY. 752 pp.

White, R., and E. Schaffer. 1980. Transient moisture gradient in fire-exposed wood slab. Wood and Fiber. 13(1):17-38.

Wilkinson, T. 1971. Theoretical lateral resistance of nailed joints. Journal of the Structural Division. ASCE. Proc. pap. 97(ST5):1381-1398.

Windholz, M. 1977. The Merck Index. Merck & Co., Inc. Rahway, N.J. 1313pp.

Wolff, E. 1988. Personal Communication.

Appendices

Appendix A. Material Property Program

```
10 REM          ****************************************
20 REM          **     FINDING JOINT PROPERTIES       **
30 REM          **        USING CUBIC SPLINE          **
35 REM          **       James Fuller  8/89           **
40 REM          ****************************************
50 DEFDBL N-Z
60 DEFDBL A-F
70 DIM Y(15,2)
80 DIM FWA(15)
90 DIM DIA(15)
100 DIM DI(15)
110 DIM H(15)
120 DIM BWA(15)
130 DIM EP(5,19)
140 DIM MP(5,19)
150 DIM TX(2,5,19)
160 DIM SM(15,15)
170 DIM T(3,15)
180 DIM P(3,15)
190 DIM A(3,15)
200 DIM B(3,15)
210 DIM C(3,15)
220 REM
230 REM        **      INPUTTING MATERIAL DATA    **
240 REM
250 OPEN "i",#1,"a:gypi"
260 FOR J = 1 TO 7
270 INPUT #1,T(1,J),P(1,J)
280 NEXT J
290 CLOSE #1
300 OPEN "i",#2,"a:woodi"
310 INPUT #2,FE
320 FOR J = 1 TO 15
330 INPUT #2,T(2,J),P(2,J)
340 NEXT J
350 CLOSE #2
360 OPEN "i",#3,"a:naili"
370 FOR J = 1 TO 7
380 INPUT #3,T(3,J),P(3,J)
390 NEXT J
400 CLOSE #3
410 FOR M = 1 TO 3
420 IF M = 2 GOTO 460
430 L = 6
440 LL = 5
450 GOTO 490
```

```
460 L = 14
470 LL = 13
480 REM
490 REM                **    finding cubic splines    **
500 REM                **      finding div diff       **
510 REM
520 FOR I = 1 TO L
530 H(I) = T(M,I+1)-T(M,I)
540 NEXT
550 FOR J = 1 TO L
560 Y(I,1) = (P(M,I)-P(M,I-1))/(T(M,I)-T(M,I-1))
570 NEXT J
580 REM
590 REM              **          cubic spline              **
600 REM              **    generating SM spline matrix     **
610 REM
620 FOR I = 3 TO LL
630 SM(I,I) = 2*(T(M,I+1)-T(M,I-1))
640 IF I = L GOTO 670
650 SM(I+1,I) = H(I)
660 SM(I,I+1) = SM(I+1,I)
670 NEXT I
680 IF M = 3 GOTO 790
690 SM(2,2) = (H(1)+H(2))*(H(1)+2*H(2))/H(2)
700 SM(2,3) = (H(2)*H(2)-H(1)*H(1))/H(2)
710 SM(3,2) = H(2)
720 IF M = 2 GOTO 760
730 SM(L,L) = 2*H(LL)+3*H(L)
740 SM(LL,L) = H(LL)
750 GOTO 850
760 SM(L,L) = (H(L)+H(LL))*(H(L)+H(LL))/H(LL)
770 SM(LL,L) = (H(LL)*H(LL)-H(L)*H(L))/H(LL)
780 GOTO 850
790 SM(2,2) = 3*H(1)+2*H(2)
800 SM(2,3) = H(2)
810 SM(3,2) = H(2)
820 SM(6,6) = 2*H(5)+3*H(6)
830 SM(5,6) = H(5)
840 REM
850 REM                **       generating D  SMxS    **
860 REM
870 FOR I = 2 TO L
880 Y(I,2) = 6*(Y(I,1)-Y(I-1,1))
890 NEXT I
900 REM
910 REM                  **     finding L    D    Lt   **
920 REM
930 Q = 0
940 FOR I = 2 TO L
```

```
950 SUM = 0
960 IF I = 2 GOTO 1000
970 FOR K = 2 TO I-1
980 SUM = SUM +SM(I,K) *SM(I,K)*DI(K)
990 NEXT K
1000 DI(I) = SM(I,I)-SUM
1010 IF I = L GOTO 1110
1020 FOR J = I+1 TO L
1030 SUM = 0
1040 IF Q = 0 GOTO 1080
1050 FOR K = 2 TO I -1
1060 SUM = SUM +SM(I,K)*SM(J,K)*DI(K)
1070 NEXT K
1080 SM(J,I) = (SM(J,I)-SUM)/DI(I)
1090 NEXT J
1100 Q = 1
1110 NEXT I
1120 REM
1130 REM                    **      forward substitution  **
1140 REM
1150 FWA(2) = Y(2,2)
1160 FOR I =3 TO L
1170 SUM = 0
1180 FOR J = 2 TO I-1
1190 SUM = SUM +SM(I,J)*FWA(J)
1200 NEXT J
1210 FWA(I) = Y(I,2) - SUM
1220 NEXT I
1230 REM
1240 REM                   **   diagonal substitution   **
1250 REM
1260 FOR I = 2 TO L
1270 DIA(I) = FWA(I)/DI(I)
1280 NEXT I
1290 REM
1300 REM                    **   backward substitution  **
1310 REM
1320 BWA(L) = DIA(L)
1330 FOR I = L TO 2 STEP -1
1340 SUM = 0
1350 FOR J = I+1 TO L
1360 SUM = SUM+SM(J,I)*BWA(J)
1370 NEXT J
1380 BWA(I) = DIA(I) -SUM
1390 NEXT I
1400 REM
1410 REM                    **   finding the coefficients  **
1420 REM
1430 FOR I = 1 TO L
```

```
1440 A(M,I) = (BWA(I+1)-BWA(I))/(6*H(I))
1450 B(M,I) = BWA(I)/2
1460 C(M,I) = (P(M,I+1)-P(M,I))/H(I)-(2*H(I)*BWA(I)+H(I)*BWA(I+1))/6
1470 NEXT I
1480 NEXT M
1490 REM
1500 REM                    **   joint temperature data input  **
1510 REM
1520 OPEN "i",#1,"a:tempi"
1530 FOR J = 1 TO 5
1540 FOR I = 1 TO 19
1550 INPUT #1,TX(1,J,I),TX(2,J,I)
1560 NEXT I
1570 NEXT J
1580 CLOSE #1
1590 REM
1600 REM                ** finding joint material properties  **
1610 REM
1620 FOR J = 1 TO 5
1630 FOR I = 1 TO 19
1640 IF I < 12 THEN M = 1 ELSE M = 2
1650 IF TX(2,J,I) > 299.9 AND M = 2 GOTO 1850
1660 IF TX(2,J,I) > 149.9 AND M = 1 GOTO 1830
1670 IF TX(2,J,I) < T(M,14) THEN K = 13 ELSE K = 14
1680 IF TX(2,J,I) < T(M,13) THEN K = 12
1690 IF TX(2,J,I) < T(M,12) THEN K = 11
1700 IF TX(2,J,I) < T(M,11) THEN K = 10
1710 IF TX(2,J,I) < T(M,10) THEN K = 9
1720 IF TX(2,J,I) < T(M,9) THEN K = 8
1730 IF TX(2,J,I) < T(M,8) THEN K = 7
1740 IF TX(2,J,I) < T(M,7) THEN K = 6
1750 IF TX(2,J,I) < T(M,6) THEN K = 5
1760 IF TX(2,J,I) < T(M,5) THEN K = 4
1770 IF TX(2,J,I) < T(M,4) THEN K = 3
1780 IF TX(2,J,I) < T(M,3) THEN K = 2
1790 IF TX(2,J,I) < T(M,2) THEN K = 1
1800 DX = TX(2,J,I)-T(M,K)
1810 EP(J,I) = P(M,K)+DX*(C(M,K)+DX*(B(M,K)+DX*A(M,K)))
1820 GOTO 1860
1830 EP(J,I) = .0133262
1840 GOTO 1860
1850 EP(J,I) = 0
1860 IF TX(1,J,I) > 625 THEN MP(J,I) = 0:GOTO 1940
1870 IF TX(1,J,I) < T(3,6) THEN K = 5 ELSE K = 6
1880 IF TX(1,J,I) < T(3,5) THEN K = 4
1890 IF TX(1,J,I) < T(3,4) THEN K = 3
1900 IF TX(1,J,I) < T(3,3) THEN K = 2
1910 IF TX(1,J,I) < T(3,2) THEN K = 1
1920 DX = TX(1,J,I)-T(3,K)
```

```
1930 MP(J,I) = P(3,K)+DX*(C(3,K)+DX*(B(3,K)+DX*A(3,K)))
1940 NEXT I
1950 NEXT J
1960 REM
1970 REM                **  saving joint material properties   **
1980 REM
1990 OPEN "o",#1,"a:joinprop"
2000 WRITE #1,FE
2010 FOR J = 1 TO 5
2020 FOR I = 1 TO 19
2030 WRITE #1,EP(J,I),MP(J,I)
2040 NEXT I
2050 NEXT J
2060 CLOSE #1
```

Appendix B. Input Data for Material Property Program

Table 6. Percent of Douglas-fir Embedment Force at 21 C (930N/cm) for Wood and Gypsum

Temperature (C)	% Embedment force wood		gypsum
	DF ‖	SPF ⊥	
21	1.00	.55	
40	.99	.543	
50	.98	.538	.03128
60	.965	.53	
75			.03742
77	.92	.505	
90			.03952
93	.835	.459	
110			.02672
120	.695	.382	
130			.01869
140	.62	.341	.01464
150	.585	.321	.0136
160	.56	.308	
182	.52	.286	
204	.465	.255	
227	.39	.214	
250	.29	.159	
283	.17	.093	

Table 7. Yielding Moment of the Nail (Ncm)

Temperature (C)	Moment
23	131.56
110	121.39
204	116.75
371	120.37
454	101.83
510	64.08
566	33.12

Table 8. Temperature Inputs for Each Time Step at Each Nodal Position (Nail,Gypsum or Wood)

Position	Temperatures (C)					
(mm)	0 min.	5 min.	10 min.	15 min.	20 min.	25 min.
0	20,20	294,300	493,500	751,760	782,789	793,800
0.38	20,20	279,285	474,476	725,731	761,773	775,785
1.27	20,20	255,225	445,425	686,667	718,740	748,753
2.54	20,20	233,162	416,369	648,603	697,690	721,717
3.81	20,20	212,135	389,284	611,545	665,637	694,685
5.08	20,20	193,121	363,267	575,490	634,596	667,652
6.35	20,20	176,112	339,229	541,439	604,557	641,619
7.62	20,20	162,105	316,198	508,394	575,519	615,587
8.89	20,20	150,100	295,175	478,350	547,483	590,558
10.1	20,20	140, 97	276,162	449,311	520,473	565,529
11.4	20,20	132, 95	258,156	423,283	494,440	541,501
12.7	20,20	124, 92	243,153	397,265	468,334	518,472
14	20,20	115, 86	224,148	369,248	439,328	490,440
15.6	20,20	105, 80	202,139	333,230	402,291	453,399
17.8	20,20	93, 72	175,121	291,208	355,271	406,357
21	20,20	81, 62	148,108	247,172	307,230	355,300
25.2	20,20	71, 54	127, 81	210,144	366,199	309,241
30.4	20,20	61, 45	109, 67	176,118	226,163	265,192
39	20,20	20, 20	30, 20	35, 40	50, 50	85,138

Appendix C. Connection Performance Program

```
1 REM          ************************************************
2 REM          **       Behavior of Nailed Connections       **
10 REM         **            James Fuller   9/89              **
20 REM         **          FINDING EMBEDMENT FORCE            **
30 REM         ************************************************
40 DIM EP(5,19)
50 DIM MP(5,19)
60 DIM INCRE(19)
70 REM               ** inputting material properties  **
80 REM               **        and distances           **
90 OPEN "i",#1,"a:joinprop"
100 INPUT #1,FE
110 FOR J = 1 TO 5
120 FOR I = 1 TO 19
130 INPUT #1,EP(J,I),MP(J,I)
140 NEXT I
150 NEXT J
160 CLOSE #1
170 OPEN "i",#1,"a:increi"
180 FOR I = 1 TO 19
190 INPUT #1,INCRE(I)
200 NEXT I
210 CLOSE #1
220 FOR J = 1 TO 5
230 GOSUB 1040
240 REM
250 REM              x2 is where gypsum moment equals
260 REM                 the nail moment
270 REM              x3 is where moment from gypsum and
280 REM                 wood equals the nail moment
290 REM              BM5 is equal the moment at the interface
300 REM              M1 is equal to 1 when the resisting moment
310 REM                 greater then the gypsum moment
320 REM              m1a is equal to 1 when the resisting moment
330 REM                 greater then the wood moment
340 REM              M3 is equal to 1 when the resisting
350 REM                 moment is greater then the nail
360 REM                 yield at x3
370 REM              m3a is 1 when the resisting moment
380 REM                  at the interface or x2 is greater
390 REM                  then the nail yielding moment
400 X2 = 0
410 X3 = 0
420 BM5 = MP(J,11)
430 M1 = 0
440 M1A = 0
```

```
450 M2 = 0
460 M3 = 0
470 M3A = 0
480 BM = 0
490 S = 0
500 DXR = 0
510 GOSUB 1550
520 IF S=0 THEN GOTO 670
530 IF BMG>BMW THEN GOTO 600
540 K =12
550 FSUMC = EFG/FE
560 KK = 19
570 BMT = 0
580 GOSUB 3050
590 IF BMR> BMG THEN M1 = 1
600 IF BMG<BMW THEN GOTO 670
610 FSUMC = EFW/FE
620 K = 1
630 KK=11
640 BMR = 0
650 GOSUB 3050
660 IF BMR> BMW THEN M1A = 1
670 IF S=0 THEN K=12:FSUMC=EFG/FE:KK=19 ELSE GOTO 710
680 BMR = 0
690 GOSUB 3050
700 IF BMR>BM5 THEN M3A= 1
710 BM = 0
720 DXR = 0
730 GOSUB 2050
740 BMR = 0
750 IF X3 = 0 GOTO 790
760 X = X3
770 GOSUB 3050
780 IF BMR>BM THEN M3=1
790 IF M1=0 AND M1A=0 AND M3=0 AND M3A=0 THEN M2=1
800 PRINT "Time interval = ",J
810 IF M1 =1 THEN PRINT "Mode 1 occurs with a force of ":
820 IF M1=2 THEN PRINT "Mode 1a occurs with a force of ":
830 IF M2 = 1 THEN PRINT "Mode 2 occurs with a force of ":
840 IF M3=1 THEN PRINT "Mode 3 occurs with a force of ":
850 IF M3A = 1 THEN PRINT "Mode 3a occurs with a force of ":
860 IF EFW<EFG THEN F=EFW ELSE F=EFG
870 PRINT USING "###.##^^^^";F
880 NEXT J
890 END
1000 REM          ****************************************
1010 REM          **    finding force and moment      **
1020 REM          **       in gypsum and wood         **
1030 REM          ****************************************
```

```
1040 K = 1
1050 KK = 11
1060 MSUM = 0
1070 FSUM = 0
1080 FOR I = K TO KK
1090 XD = INCRE(I)-INCRE(I-1)
1100 FSUM = EP(J,I)*XD+FSUM
1110 IF K = 1 THEN Y = .5-INCRE(I) ELSE Y = INCRE(I-1)-.5
1120 MSUM = EP(J,I)*XD*(Y+.5*XD)+MSUM
1130 NEXT I
1140 EFW= FE*FSUM
1150 BMW = MSUM*FE
1160 IF K = 1 THEN EFG = EFW:BMG = BMW ELSE RETURN
1170 K = 12
1180 KK = 19
1190 GOTO 1060
1500 REM      ************************************************
1510 REM      **          finding where moments equals      **
1520 REM      **                 nail yield                 **
1530 REM      **            for less then 12.7 mm           **
1540 REM      ************************************************
1550 K = 1
1560 MSUM = 0
1570 FSUM = 0
1580 BML = BM
1590 FOR I = 1 TO K
1600 XD = INCRE(I)-INCRE(I-1)
1610 FSUM = FSUM+EP(J,I)*XD
1620 MSUM = EP(J,I)*XD*(INCRE(K)-INCRE(I)+.5*XD)+MSUM
1630 NEXT I
1640 BM = FE*MSUM
1650 IF BM = MP(J,K) AND BM > 0 THEN RETURN
1660 IF BM > MP(J,K) AND MP(J,K) > 0 THEN RETURN
1670 IF INCRE(K) = .5 THEN S=1:RETURN
1680 K = K+1
1690 GOTO 1560
2000 REM        ************************************************
2010 REM        **         finding where moment equals        **
2020 REM        **                nail yield                  **
2030 REM        **          for greater then 12.7 mm          **
2040 REM        ************************************************
2050 K = 12
2060 FSUM = 0
2070 MSUM = 0
2080 BML = BM
2090 FOR I = 1 TO 11
2100 XD = INCRE(I)-INCRE(I-1)
2110 FSUM = FSUM+EP(J,I)*XD
2120 MI = EP(J,I)*XD*(X-INCRE(I)+.5*XD)
```

```
2130 MSUM = MSUM + MI
2140 NEXT I
2150 FOR I = 12 TO K
2160 XD = INCRE(I)-INCRE(I-1)
2170 FSUM = FSUM-EP(J,I)*XD
2180 MI = EP(J,I)*XD*(INCRE(K)-INCRE(I)+.5*XD)
2190 MSUM = MSUM - MI
2200 NEXT I
2210 BM = FE*MSUM
2220 X = INCRE(K)
2230 IF BM > MP(J,K) AND MP(J,K) > 0 THEN GOTO 2330
2240 IF BM = MP(J,K) AND BM>0 THEN X3 = INCRE(K):RETURN
2250 K = K+1
2260 IF K = 19 THEN RETURN
2270  GOTO 2060
2280 REM
2290 REM              **   finding where My equals   **
2300 REM              **   nail yield exactly for    **
2310 REM              **   greater then 12.7 mm      **
2320 REM
2330 NMP = MP(J,K)
2340 NEP = EP(J,K)
2350 K = K-1
2360 E = NMP/BM
2370 G = 0
2380 IF E < 1.1 AND E > .9 THEN X3 = X:RETURN
2390 G = 1
2400 IF E >1.1 THEN FAC = 1.5 ELSE FAC = 1
2410 FRAC = FAC*(NMP-BML)/(BM-BML)
2420 NMP = FRAC*(NMP-MP(J,K))+MP(J,K)
2430 DX = FRAC*(X-INCRE(K))
2440 NEP = FRAC*(NEP-EP(J,K))+EP(J,K)
2450 X = DX+INCRE(K)
2460 BML = BM
2470 FSUM = 0
2480 MSUM = 0
2490 FOR I = 1 TO 11
2500 XD = INCRE(I)-INCRE(I-1)
2510 FSUM = FSUM+EP(J,I)*XD
2520 MI = EP(J,I)*XD*(X-INCRE(I)+.5*XD)
2530 MSUM = MSUM + MI
2540 NEXT I
2550 FOR I = 12 TO K
2560 XD = INCRE(I)-INCRE(I-1)
2570 FSUM = FSUM-EP(J,I)*XD
2580 MI = EP(J,I)*XD*(X-INCRE(I)+.5*XD)
2590 MSUM = MSUM - MI
2600 NEXT I
2610 FSUM = FSUM-DEP*DX
```

```
2620 MI = DEP*DX*DX*.5
2630 MSUM = MSUM - MI
2640 BM = FE*MSUM
2650 GOTO 2360
2660 IF G = 1 THEN DXR=INCRE(K+1)-X:K=K+2 ELSE K=K+1
2670 FSUMC= FSUM-EP(J,K+1)*DXR
2680 RETURN
3000 REM      ***************************************************
3010 REM      **     finding the resisting bending moment      **
3020 REM      ***************************************************
3030 REM                  **  finding force center    **
3040 REM
3050 C = K-1
3060 FSUML = FSUM
3070 FSUM = FSUMC
3080 IF C = K-1 GOTO 3120
3090 FOR I = K TO C
3100 FSUM = FSUM-EP(J,I)*(INCRE(I)-INCRE(I-1))
3110 NEXT I
3120 FOR III = C+1 TO KK
3130 FSUM = FSUM+EP(J,III)*(INCRE(III)-INCRE(III-1))
3140 NEXT III
3150 IF FSUM = 0 THEN NX = INCRE(C):GOTO 3560
3160 IF FSUM < 0 THEN GOTO 3250
3170 IF C = 19 THEN RETURN
3180 FX = INCRE(C)
3190 FEP = EP(J,C)
3200 C = C+1
3210 GOTO 3060
3220 REM
3230 REM                 **    FINDING EXACT FORCE CENTER  **
3240 REM
3250 SX = INCRE(C)
3260 SEP = EP(J,C)
3270 C =C -1
3280 PER = ABS(SX/(SX-FX))
3290 IF PER <.005 THEN GOTO 3560
3300 IF PER< .995 THEN GOTO 3340
3310 NX = SX
3320 NEP = SEP
3330 GOTO 3560
3340 NEP = (SEP-FEP)*PER+FEP
3350 NX = FX+(SX-FX)*PER
3360 FSUMI = FSUMC
3370 FOR I = K TO C
3380 FSUMI= FSUMI-EP(J,I)*(INCRE(I)-INCRE(I-1))
3390 NEXT I
3400 FSUMI= FSUMI-(NX-FX)*NEP+(INCRE(C+1)-NX)*EP(J,C+1)
3410 FOR III = C+2 TO KK
```

```
3420 FSUMI= FSUMI+EP(J,III)*(INCRE(III)-INCRE(III-1))
3430 NEXT III
3440 IF FSUMI> 0 GOTO 3490
3450 FSUM = FSUMI
3460 SX = NX
3470 SEP = NEP
3480 GOTO 3280
3490 FSUML = FSUMI
3500 FEP = NEP
3510 FX = NX
3520 GOTO 3280
3530 REM
3540 REM                    ** finding  the moment  **
3550 REM
3560 MRSUM = 0
3570 FOR I = K TO C
3580 DX = INCRE(I)-INCRE(I-1)
3590 MRSUM = MRSUM-EP(J,I)*DX*(INCRE(I)-X-.5*DX)
3600 NEXT I
3610 FOR I = C+2 TO KK
3620 DX = INCRE(I)-INCRE(I-1)
3630 MRSUM = MRSUM+EP(J,I)*DX*(INCRE(I)-X-.5*DX)
3640 NEXT I
3650 DX2 = INCRE(C+1)-NX
3660 MRSUM = MRSUM+EP(J,C+1)*DX2*(INCRE(C+1)-X-.5*DX2)
3670 MRSUM = MRSUM-NEP*(NX-FX)*(INCRE(C)-X+.5*(NX-FX))
3680 BMR = ABS(MRSUM*FE)
3690 RETURN
```

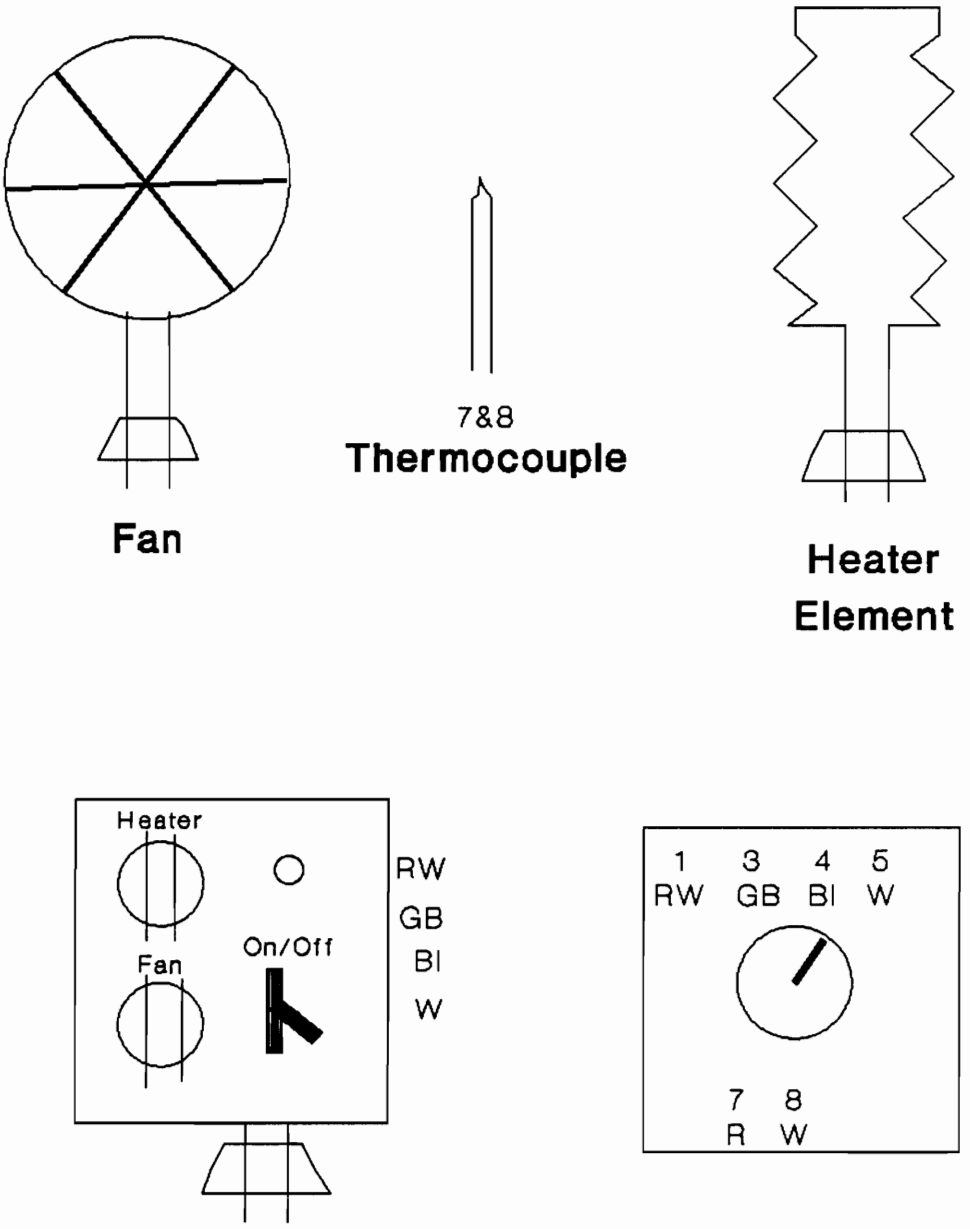

Figure 19. Electrical Components and Wiring Terminals for the Testing Chamber